

RESEARCH

Open Access



# Human umbilical cord/placenta mesenchymal stem cell conditioned medium attenuates intestinal fibrosis in vivo and in vitro

Yoon Jeong Choi<sup>1,2</sup>, Woo Ram Kim<sup>3</sup>, Duk Hwan Kim<sup>1</sup>, Jee Hyun Kim<sup>1\*</sup>  and Jun Hwan Yoo<sup>1,2\*</sup>

## Abstract

**Background** A significant unmet need in inflammatory bowel disease is the lack of anti-fibrotic agents targeting intestinal fibrosis. This study aimed to investigate the anti-fibrogenic properties and mechanisms of the conditioned medium (CM) from human umbilical cord/placenta-derived mesenchymal stem cells (UC/PL-MS-CM) in a murine intestinal fibrosis model and human primary intestinal myofibroblasts (HIMFs).

**Methods** UC/PL-MS-CM was concentrated 15-fold using a 3 kDa cut-off filter. C57BL/6 mice aged 7 weeks old were randomly assigned to one of four groups: (1) control, (2) dextran sulfate sodium (DSS), (3) DSS + CM (late-phase treatment), and (4) DSS + CM (early-phase treatment). Chronic DSS colitis and intestinal fibrosis was induced by three cycles of DSS administration. One DSS cycle consisted of 7 days of oral DSS administration (1.75%, 2%, and 2.5% DSS), followed by 14 days of drinking water. UC/PL-MS-CM was intraperitoneally administered in the late phase (from day 50, 10 times) or early phase (from day 29, 10 times) of DSS cycles. HIMFs were treated with TGF- $\beta$ 1 and co-treated with UC/PL-MS-CM (10% of culture media) in the cellular model.

**Results** In the animal study, UC/PL-MS-CM reduced submucosa/muscularis propria thickness and collagen deposition, which improved intestinal fibrosis in chronic DSS colitis. The UC/PL-MS-CM significantly reduced the expressions of procollagen1A1 and  $\alpha$ -smooth muscle actin, which DSS significantly elevated. The anti-fibrogenic effect was more apparent in the UC-MS-CM or early-phase treatment model. The UC/PL-MS-CM reduced procollagen1A1, fibronectin, and  $\alpha$ -smooth muscle actin expression in HIMFs in the cellular model. The UC/PL-MS-CM downregulated fibrogenesis by suppressing RhoA, MRTF-A, and SRF expression.

**Conclusions** Human UC/PL-MS-CM inhibits TGF- $\beta$ 1-induced fibrogenic activation in HIMFs by blocking the Rho/MRTF/SRF pathway and chronic DSS colitis-induced intestinal fibrosis. Thus, it may be regarded as a novel candidate for stem cell-based therapy of intestinal fibrosis.

**Keywords** Intestinal fibrosis, Conditioned medium, Mesenchymal stem cells, Umbilical cord, Placenta

<sup>†</sup>Jee Hyun Kim and Jun Hwan Yoo contributed equally to this work.

\*Correspondence:

Jee Hyun Kim

miji2120@gmail.com

Jun Hwan Yoo

jhyoo@cha.ac.kr

Full list of author information is available at the end of the article



## Background

Intestinal fibrosis is a significant complication of inflammatory bowel disease (IBD) and is more common in Crohn's disease (CD) than in ulcerative colitis [1]. Over 50% of patients with CD exhibit fibrotic complications, most notably stricture and penetration, which result in potential intestinal obstruction and require surgical intervention [2]. Fibrostenosis caused by stricture formation remains a significant challenge in the management of patients with IBD, and few effective anti-fibrotic therapies are currently available. Most IBD treatments aim to reduce inflammation; however, treatments specifically targeting intestinal fibrosis are limited. Moreover, while it was long believed that suppressing chronic inflammation might prevent fibrosis, recent studies have revealed that it could persist even without inflammation [3]. Therefore, it is critical to develop anti-fibrotic agents that directly target intestinal fibrosis for the treatment of patients with CD and related gastrointestinal (GI) disorders.

The pathogenesis of intestinal fibrosis is a complex process that is not fully understood. Fibrosis is characterized by excessive deposition of extracellular matrix (ECM) proteins, including collagen and fibronectin, produced by activated myofibroblasts [4]. Activated myofibroblasts play a critical role in fibrosis development. These myofibroblasts express elevated levels of  $\alpha$ -smooth muscle actin ( $\alpha$ -SMA) and contribute to tissue distortion and intestinal strictures via ECM contraction [5]. Transforming growth factor (TGF- $\beta$ 1) is a crucial pro-fibrotic cytokine that stimulates fibrogenic myofibroblast activation [6, 7]. TGF- $\beta$ 1-induced fibrogenic activation occurs via Smad-dependent and -independent signaling pathways [8–10]. The RhoA/ROCK signaling pathway is critical in regulating actin cytoskeleton dynamics and transcriptional responses in numerous cell types, including fibrotic myofibroblasts. Activated RhoA triggers ROCK activation, promoting globular-actin (G-actin) polymerization into filamentous actin (F-actin), forming actin stress fibers and leading to contractile force generation by myofibroblasts. Moreover, the RhoA/ROCK signaling pathway regulates pro-fibrotic gene expression by promoting nuclear translocation of myocardin-related transcription factor A (MRTF-A), a co-activator of serum response factor (SRF), which is a transcription factor that regulates the expression of genes involved in cell proliferation and differentiation, including those that promote fibrosis [9, 11]. Further, when G-actin polymerizes into F-actin, MRTF-A is liberated from G-actin, allowing it to translocate to the nucleus and bind to SRF, thereby activating the transcription of pro-fibrotic genes.

Mesenchymal stem cells (MSCs) suppress the inflammatory response by secreting anti-inflammatory cytokines and regulating the immune system. They also

have anti-fibrotic properties because they reduce the deposition of ECM and fibrosis-associated factors in tissues [12–16]. Several preclinical studies have found that MSCs can alleviate fibrosis in multiple organs, including the liver, lungs, kidneys, heart, skin, peritoneum, pancreas, and colorectum [17–22]. Umbilical cord and placenta-derived mesenchymal stem cells (UC/PL-MSCs) have gained attention as a promising alternative to traditional MSC populations for clinical applications owing to their ability to be obtained in larger quantities without invasive procedures and their higher proliferation and differentiation potential. Our previous study has revealed that UC/PL-MSCs have therapeutic potential by suppressing TGF- $\beta$ 1-induced fibrogenic activation in human primary intestinal myofibroblasts (HIMFs) [23].

The risk of vascular occlusion and malignant transformation following direct administration is important when considering the therapeutic use of MSCs [24–26]. There is increasing interest in investigating conditioned medium (CM) containing various biologically active molecules and extracellular vesicles (EVs) secreted by MSCs. Several enzymes involved in ECM-remodeling, such as matrix metalloproteinases (MMP2 and MMP9) and their inhibitors TIMP-1 and TIMP-2 have been found in MSC-CM [27–29]. In addition, anti-fibrogenic cytokines, such as interleukin-10 (IL-10) and prostaglandin-E2, as well as growth factors, such as vascular endothelial growth factor and hepatocyte growth factor (HGF), have been found. In addition to proteins, MSC-CM contains microRNAs with anti-fibrotic properties [30–32]. Owing to the ability of the CM to induce tissue regeneration and modulate the immune response, it is now considered a viable strategy for MSC-based therapy.

In this study, the anti-fibrotic effects and mechanisms of action of the CM derived from human UC/PL-MSCs (UC/PL-MSC-CM) in intestinal fibrosis were evaluated in a murine model of chronic colitis caused by dextran sodium sulfate (DSS) and in HIMFs. The results of this study provide new insights into the potential clinical use of UC/PL-MSC-derived products for treating fibrotic diseases of the intestine.

## Materials and methods

### Mice and reagents

Female C57BL/6 wild-type mice were purchased from Orient (Seongnam, Korea) and used under specific pathogen-free conditions. The mice were given access to standard chow and sterile water ad libitum until they grew to the desired age (7–8 weeks) and body weight (19–22 g). DSS was purchased from MP Biochemicals (Irvine, CA, USA). Recombinant human TGF- $\beta$ 1 was obtained from R&D systems (Minneapolis, MN). The ethics committee at CHA University assessed and approved the procedures

for conducting this animal study (IACUC210145). All experimental procedures in the animal study were performed in accordance with NIH guidelines.

#### Preparation of human UC/PL-MSCs

CHA Biotech, Co. Ltd. (Seongnam, Korea) provided human umbilical cord- and placenta-derived MSCs. The isolation and expansion of human UC/PL-MSCs were performed according to the Good Clinical Practice guidelines of the Master Cell Bank. Further the preparations of the human UC/PL-MSCs were conducted in the Good manufacturing practices facility. The preparation and characterization of the cells have been described previously [23, 33–35]. Umbilical cord and placenta tissue were obtained with informed consent from healthy mother donors at CHA Bundang Medical Center (Seongnam, Korea). After severing the umbilical vessels, Wharton's jelly was sliced into 1–5 mm explants to isolate UC-MSC. Isolated slices were attached to culture plates and subsequently cultured in  $\alpha$ -modified minimal essential medium ( $\alpha$ -MEM; Hyclone) supplemented with 10% fetal bovine serum (FBS; Gibco), 25 ng/mL fibroblast growth factor-4 (FGF4; Peprotech, London, England), 1  $\mu$ g/mL heparin (Sigma, St. Louis, MO), and 0.5% gentamycin (Gibco) at 37 °C in a humidified atmosphere containing 5% CO<sub>2</sub>. Every 3 d, the medium was changed and on day 6, the UC-MSC cell populations emerged as outgrowths from the UC fragments. The umbilical cord fragments were discarded after 15 d, and the cells were grown until sub-confluence (80–90%) using TrypLE (Invitrogen, Carlsbad, CA). UC-MSCs at passage six were used, as described in our previous study, and the phenotype of the cells was determined using fluorescence-activated cell sorting (FACS) analysis [23].

The placental membranes were bluntly dissected from the placental body and then washed in Dulbecco's phosphate-buffered saline (Gibco) to remove the blood from isolated the PL-MSCs. The amniotic connective tissue of the placental membranes was carefully harvested using two slide glasses and then incubated at 37 °C with shaking (175 rpm) for 15 min with HBSS containing 1 mg/

mL type I collagenase (Sigma), 1.2 U/mL dispase (Gibco), 2 mg/mL trypsin (Sigma), 65  $\mu$ g/mL DNase I (Roche, Mannheim, Germany), and 1  $\times$  penicillin–streptomycin (Gibco). The viability of the isolated cells was determined by trypan blue exclusion. PL-MSCs were cultured in  $\alpha$ -MEM (Hyclone) supplemented with 10% FBS (Gibco), 25 ng/mL FGF4 (Peprotech), 1  $\mu$ g/mL heparin (Sigma), and 0.5% gentamycin (Gibco) at 37 °C in a humidified atmosphere containing 5% CO<sub>2</sub>. FACS analysis was used to identify the phenotype of the cells, and the PL-MSCs at passage six were used in this study [23].

#### Preparation of CM from human UC/PL-MSCs

A total of  $1.0 \times 10^6$  UC/PL-MSCs were seeded in a 100 mm dish (in 10 mL UC/PL-MSCs culture medium) to prepare the CM. The serum-free HIMFs culture medium was then replaced after 24 h. After incubating UC/PL-MSCs for 72 h, the CM was harvested. Cell debris was then removed by centrifuging the medium at  $3800 \times g$  for 10 min. The supernatant was collected, filtered through a 0.2  $\mu$ m filter, and then concentrated 15-fold using a 3-kDa cut-off centrifugal filter (Amicon Ultra, Merck Millipore, Burlington, MA, USA) at  $4000 \times g$  for 40 min at 4 °C.

#### Co-culture of HIMFs with UC/PL-MSC-CM

HIMFs grown in the presence of serum were starved for 24 h in HIMF serum-free medium before being treated with 5 ng/mL TGF- $\beta$ 1 alone or in combination with 10% UC/PL-MSC-CM to investigate the effects of UC/PL-MSC-CM on TGF- $\beta$ 1-mediated HIMFs fibrosis.

#### Induction of DSS-induced fibrosis and UC/PL-MSC-CM treatment

Mice were subjected to repeated "cycles" of DSS administration to evaluate chronic colitis and fibrosis (Fig. 1A). One cycle was defined as a 7 d exposure to DSS, followed by a two-week recovery phase with normal drinking water. Mice were subjected to three cycles: one (1.75% DSS), two (2% DSS), and three (2.5% DSS). Control mice received normal drinking water. Two experimental groups were used to evaluate the anti-fibrotic effects

(See figure on next page.)

**Fig. 1** UC/PL-MSC-CM exhibits protective effects on the clinical course of chronic DSS-induced colitis. **A** Experimental design of repeated "cycles" of DSS exposure, as described in the "Methods" section. Mice were randomized into four groups: (1) control group (water-treated mouse group,  $n = 15$ ); (2) DSS group (DSS and vehicle-treated mouse group,  $n = 15$ ); (3) UC/PL-MSC-CM-Exp. 1 group (DSS and UC/PL-MSC-CM-treated mouse group according to Exp. 1 schedule,  $n = 10$ ); and (4) UC/PL-MSC-CM-Exp. 2. (DSS and UC/PL-MSC-CM-treated mouse group according to Exp. 2 schedule,  $n = 15$ ). Three DSS administration cycles induced chronic DSS colitis and intestinal fibrosis. One DSS cycle comprised of 7 d oral administration of DSS (1.75%, 2%, and 2.5% DSS), followed by 14 d of water drinking. In Exp. 1, the UC/PL-MSC-CM was injected intraperitoneally ten times during the late phase of the DSS cycles, starting from day 50. In Exp. 2, the UC/PL-MSC-CM was administered ten times during the early phase of the DSS cycles, starting from day 29. **B** Relative weight curve. **C** Relative weight at day 64. **D** Macroscopic appearance of the colons from the mice. **E** Colon length, colon weight, and colon weight/colon length of mice. Data are expressed as means  $\pm$  SEM ( $n = 10$ –15 in each group).  $^{###}P < .001$  versus the control group;  $^*P < .05$ ,  $^{**}P < .01$  and  $^{***}P < .001$  versus the DSS group (ANOVA w/ Tukey)

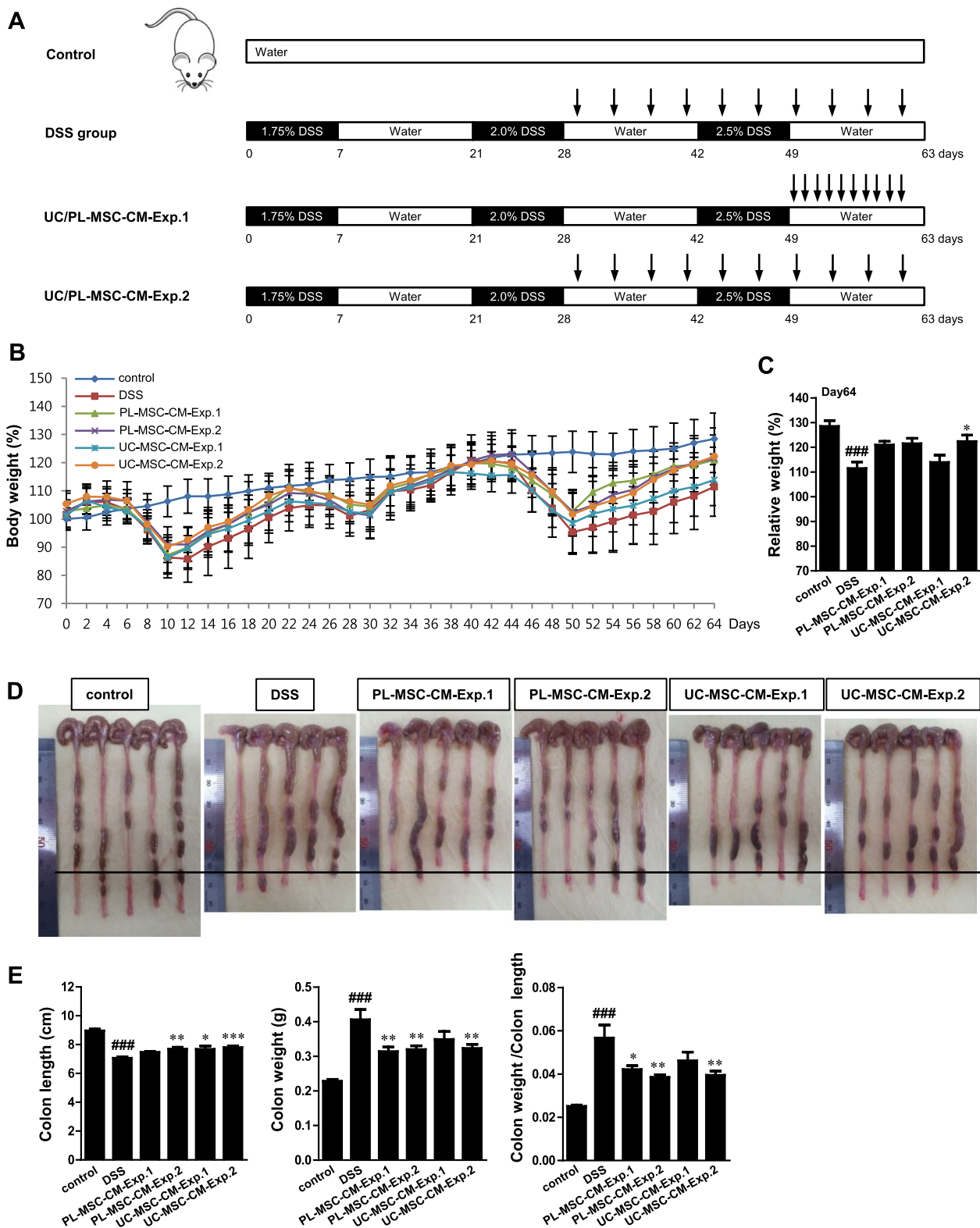


Fig. 1 (See legend on previous page.)

of UC/PL-MSC-CM in an early- (Exp. 1) and late-phase treatment model (Exp. 2). In Exp. 1, we administered 150 µg/100 µL/mouse of UC/PL-MSC-CM intraperitoneally daily from Day 50 to Day 59. In Exp. 2, we administered 150 µg/100 µL/mouse of UC/PL-MSC-CM intraperitoneally twice weekly from Day 29 to Day 61. Four groups of mice were randomly assigned: (1) control group (water-treated mouse group, n = 15); (2) DSS group (DSS and vehicle-treated mouse group, n = 15); (3) UC/PL-MSC-CM-Exp. 1 group (DSS and UC/PL-MSC-CM-treated mouse group according to Exp. 1 schedule, n = 10); and (4) UC/PL-MSC-CM-Exp. 2 (DSS and UC/PL-MSC-CM-treated mouse group according to Exp. 2 schedule, n = 15). All experiments were performed in the same timeframe. On day 64, all mice were euthanized by CO<sub>2</sub> asphyxiation.

#### Macroscopic assessment and evaluation of fibrosis

Mice were weighed for body weight changes. After the mice were euthanized, the colon was removed entirely, and the length and weight were measured. The length from cecum to the anus was used to determine the length of the colon. The complete mouse colon was excised for historical analysis, and segments of the transverse tissues (1 cm) were then fixed in 10% buffered formalin, paraffin-embedded, and stained with hematoxylin and eosin. Zeiss Axio Scan.Z1 slide scanner was used to collect and digitize all histological sections, and ZEN 3.1 (blue edition) software was used for analysis. The thickness of the mucosa and muscularis propria of each mouse was calculated as the mean value of five distinct points. Sirius red staining (ab150681, abcam) was used to evaluate fibrosis. A hydroxyproline assay kit (ab222941, abcam) was used to obtain the collagen in the tissue according to the protocol of the manufacturer. A Zeiss Axio Scan.Z1 slide scanner was used to read the stained sections. Using ZEN 3.1 (blue edition) software, the quantified outcomes of Sirius red staining were presented as the mean density of five randomly selected fields from each group.

#### Immunohistochemical analysis

Paraffin sections were deparaffinized in xylene and then hydrated in a graded ethanol series to evaluate the expression of Procoll1A1 and α-SMA in colon tissues. REAL Peroxidase-Blocking Solution (S2023, DAKO, Carpinteria, CA, USA) was used to block the endogenous peroxidase activity for 30 min before masked antigens were retrieved using a 10 mM sodium citrate buffer at 95 °C for 1 h. Tissue slices were blocked with Protein Block solution (X0909, DAKO, Carpinteria, CA, USA) for 30 min before being incubated with a primary antibody at 4 °C overnight. The secondary antibody that was peroxidase-conjugated (#31430, Invitrogen) was incubated

for 30 min at room temperature. All specimens were color developed using the DAB Substrate Kit (ab64238, Abcam, Cambridge, MA, USA) and counterstained with hematoxylin after being rinsed with PBS. The stained sections were read under a Zeiss Axio Scan.Z1 slide scanner and they were quantified using ZEN 3.1 (blue edition) software. The quantified results of Procoll1A1 and α-SMA expression were presented as the mean density of five randomly selected fields from each group.

#### Human intestinal myofibroblast isolation and culture

Primary HIMFs were isolated and cultured as per a previously described protocol with some modifications [36]. Briefly, HIMFs were derived from the outgrowths of minced colonic mucosa explants placed on etched polystyrene flasks containing HIMFs growth medium consisting of Dulbecco's modified Eagle's medium/high glucose (Hyclone, Logan, UT), 10% FBS (American Type Culture Collection, Manassas, VA), 4 mmol/L L-glutamine (Gibco, Carlsbad, CA), 25 mmol/L HEPES, 100 U/mL penicillin, 100 µg/mL streptomycin, and 0.25 µg/mL amphotericin B (all purchased from Lonza, Walkersville, MD) and used between passages 6 and 10 at 80% confluence. HIMFs were isolated from normal colon segments of patients undergoing resection for colorectal cancer. Following surgical resection, a pathologist removed the segments of the colon that were grossly normal from the area near the proximal resection margin. The periphery of the normal colon segments, which was used for isolation, was histologically confirmed under a microscope. The project was performed in accordance with the guidelines of the Institutional Review Board of the CHA Bundang Medical Center.

#### RNA isolation and real-time quantitative PCR (RT-qPCR)

TRIzol reagent (Ambion, Carlsbad, CA) was used to extract RNA from the HIMFs. The ReverTra Ace qPCR RT Master Mix Kit (TOYOBO, Osaka, Japan) was then used to reverse-transcribe an identical amount of RNA (1 g) into cDNA according to the instructions of the manufacturer. All RT-qPCR reactions were performed using a Roche Light Cycler 96 instrument (Roche) with Faster-Start Essential DNA Probes Master (Roche). All gene mRNA levels were normalized to GAPDH levels. The specific primers for the collagen1A1 (Hs00164004\_m1), fibronectin (Hs01549976\_m1), α-SMA (ACTA2, Hs00426835\_g1), Mkl1 (MRTF-A, Hs01090249\_g1), SRF (Hs01065256\_m1), RhoA (Hs00357608\_m1), Rock1 (Hs01127701\_m1), Rock2 (Hs00178154\_m1), and GAPDH (Hs03929097\_g1) genes were purchased from Applied Biosystems (Foster City, CA).

### Western blot

RIPA buffer (Cell Signaling, Beverly, MA) was used to isolate protein extracts. Protein samples were mixed with an equal volume of 5×SDS sample buffer to separate on 10% SDS-PAGE gels after boiling for 5 min. The proteins were then transferred to polyvinylidene difluoride membranes following electrophoresis. Next, the membranes were blocked for 1 h at room temperature with 5% nonfat dry milk in Tris-buffered saline with Tween-20 buffer (TBS-T). Membranes were incubated with specific antibodies overnight at 4 °C. After three TBS-T washes to remove the primary antibodies, the membranes were treated for 2 h with horseradish peroxidase-conjugated anti-rabbit or anti-mouse immunoglobulin (GeneTex, Irvine, CA). Following three washes with TBS-T, antigen-antibody complexes were identified using the Super-Signal West Pico Chemiluminescence System (Thermo Fisher Scientific, Rockford, IL). A luminous image analyzer (ChemiDoc™ XRS+ System, Bio-Rad, USA) was used to acquire the signals. ImageJ 1.50i software (Wayne Rasband, National Institute of Health, USA) was used to quantify the western blots. The following antibodies were used: procollagen1A1 (Procoll1A1) antibody (SP1D8, Developmental Studies Hybridoma Bank, Iowa City, IA) and fibronectin (FN) antibody (ab2413, Abcam, Cambridge, MA). Others include  $\alpha$ -smooth muscle actin ( $\alpha$ -SMA) antibody (A2547, Sigma), phospho-Smad2 (Ser465/467) antibody (#3108, Cell Signaling), RhoA antibody (#sc-418, Santa Cruz Biotechnology, Dallas, TX), GAPDH antibody (#2118, Cell Signaling), Mkl1(MRTF-A) antibody (21166-1-AP, ProteinTech), SRF antibody (#5147, Cell Signaling), and HDAC1 antibody (#5356, Cell Signaling).

### Immunocytochemistry

As previously mentioned, immunofluorescence staining was performed [7]. To evaluate the anti-fibrogenic properties of the UC/PL-MSC-CM, HIMFs ( $1.0 \times 10^4$  cells/well) were seeded onto the chamber slides (#30108, SPL life Sciences, Korea) and exposed to TGF- $\beta$ 1 (5 ng/mL) co-incubated with or without UC/PL-MSC-CM for 48 h before being fixed with 4% paraformaldehyde for 10 min. The cells were treated with primary antibodies at 4 °C overnight after permeabilization with 0.1% Triton X-100 in 1×PBS and blocking with 5% bovine serum albumin. The western blot contains information on all antibodies employed in immunocytochemistry. After three PBS washes (10 min each), the cells were incubated for 2 h at room temperature with AlexaFluor488/594-conjugated goat anti-mouse/rabbit secondary antibody (Molecular Probes, Eugene, OR). After washing, the cells were mounted using Fluoroshield Mounting Medium with DAPI (ab104139, Abcam) and examined using a Zeiss

LSM880 confocal laser scanning microscope with the appropriate fluorescent filter.

Images were imported into the ImageJ software to quantify the nuclear-to-cytoplasmic ratio. Individual cells were defined with the Cell Mask dye, and the optical density of the MRTF-A staining was assessed and adjusted for cell area. The DAPI stain was then used to delineate the nucleus and calculate the density of the MRTF-A staining within it. Subtracting the nuclear fraction from the total cell calculation yielded the cytoplasmic fraction. The nuclear-to-cytoplasmic ratio was calculated by dividing the nuclear signal by the cytoplasmic signal.

### Extraction of nuclear and cytoplasmic proteins

Nuclear and cytoplasmic fractions of the HIMFs were extracted using the Nuclear Extraction kit (Millipore) according to the protocol of the manufacturer. The protein concentration was then determined using the bicinchoninic acid protein assay, followed by western blotting.

### Statistical analysis

The mean  $\pm$  standard error of the mean of at least three independent experiments is used to express the data. The Mann-Whitney U test was used to compare the two groups. Analysis of variance with Tukey's post hoc test was performed for multiple comparisons. Statistical significance was defined as  $P$ -values  $< 0.05$ . GraphPad Prism 8.0 (GraphPad, San Diego, CA, USA) was used for all statistical analyses.

## Results

### UC/PL-MSC-CM demonstrates protective effects on the clinical course of chronic DSS-induced colitis

A murine fibrosis model was constructed using repeated cycles of DSS exposure to explore the therapeutic effect of the human UC/PL-MSC-CM in chronic colitis. Two experiments, UC/PL-MSC-CM-Exp. 1 and UC/PL-MSC-CM-Exp. 2, were designed to assess the effects of UC/PL-MSC-CM treatment. In UC/PL-MSC-CM-Exp. 1, mice received daily intraperitoneal injections of UC/PL-MSC-CM (150  $\mu$ g/100  $\mu$ L/mouse) from Day 50 to Day 59, while UC/PL-MSC-CM-Exp. 2 involved twice-weekly intraperitoneal injections (150  $\mu$ g/100  $\mu$ L/mouse) from Day 29 to Day 61 (Fig. 1A). The findings revealed that weight loss in mice repeatedly exposed to DSS began on Day 6 and gradually recovered (Fig. 1B). Both UC/PL-MSC-CM-Exp. 1 and Exp. 2 groups exhibited less weight loss compared to the DSS group, with UC-MSC-CM-Exp. 2 showing a significant reduction in weight loss on Day 64 (Fig. 1C). In both Exp. 1 and Exp. 2 groups, treatment with PL-MSC-CM demonstrated a tendency towards a reduction in weight loss; however, this trend did not reach statistical significance. To evaluate the

presence and extent of inflammation and fibrosis, the parameters of colon weight, length, and the weight-to-length ratio were systematically examined. DSS exposure significantly decreased colon length (Fig. 1D, E), indicating that DSS caused severe intestinal inflammation and fibrosis. However, in Exp. 2, UC/PL-MSC-CM treatment significantly reversed colon shortening in DSS-exposed mice. Furthermore, a significant increase in colon weight was observed in mice subjected to DSS treatment. In contrast, there was a notable decrease in colon weight in the PL-MSC-CM-Exp. 1 group and the UC/PL-MSC-CM-Exp. 2 group. Additionally, when compared with the DSS-treated group, the mice in both the PL-MSC-CM-Exp. 1 and UC/PL-MSC-CM-Exp. 2 groups exhibited significantly reduced colon weight-to-length ratios.

#### UC/PL-MSC-CM ameliorates inflammation-associated intestinal fibrosis in chronic DSS-induced colitis

Chronic DSS exposure can cause chronic intestinal inflammation and lead to various complications, including aberrant epithelial structure, thicker gut wall, persistent collagen deposition, and mononuclear cell infiltration. Histological analysis showed that UC/PL-MSC-CM treatment significantly reduced colonic injury compared to the DSS group (Fig. 2A). Specifically, UC-MSC-CM-Exp. 1 and UC/PL-MSC-CM-Exp. 2 treatments protected the extension of crypt distortion while ameliorating inflammatory reactions such as mucosal and submucosal infiltrations. Furthermore, the thickness of the submucosa and muscularis propria increased significantly in the DSS group, followed by a significant decrease after treatment with UC-MSC-CM in Exp. 1 and UC/PL-MSC-CM in Exp. 2 (Fig. 2B, C).

Sirius red staining, a technique for histological analysis, was employed to visualize the accumulation of collagen in the mucosal and submucosal layers, indicative of fibrosis, in mice with chronic colitis. The results showed that administration of UC/PL-MSC-CM in Exp. 1 and Exp. 2 had a protective effect against fibrosis-associated collagen deposition (Fig. 2D, E). In addition, we assessed the levels of hydroxyproline (collagen metabolites) to assess the severity of colon fibrosis. The hydroxyproline concentration was found to be significantly higher in the DSS-treated group when compared to the control group. Conversely, in the UC-MSC-CM-Exp. 2 group, this concentration was significantly lower (Fig. 2F).

Biomarkers such as Procol1A1 and  $\alpha$ -SMA are commonly utilized for the evaluation of intestinal fibrosis. The administration of DSS resulted in a significant increase in the expression levels of both Procol1A1 and  $\alpha$ -SMA, as shown in Fig. 3. Notably, in Exp. 2, treatment with UC-MSC-CM led to a significant reduction in Procol1A1 expression (Fig. 3A, C). Furthermore, the expression of

$\alpha$ -SMA was significantly decreased following UC/PL-MSC-CM treatment in both Exp. 1 and Exp. 2 (Fig. 3B, D). RT-qPCR analysis was used to evaluate the colonic mRNA expression of fibrosis-related genes (*Col1a1*, *Fn1*, *Acta2*, *Col3a1*, *Tnfa*, *Tgfb1*, *Ccn2*, *Mmp2*, *Mmp9*, and *Timp1*) (Additional file 1: Fig. S1 and Additional file 2). In Exp. 2, UC-MSC-CM significantly reduced the rise in *Tnfa* mRNA expression observed in the DSS group. In Exp. 2, treatment with UC-MSC-CM exhibited a trend towards the reduction in the mRNA expression levels of *Acta2*, *Tgfb1*, *Mmp9*, and *Timp1*. However, these observed changes did not achieve statistical significance. These observations lend further support to the hypothesis that UC/PL-MSC-CM has a beneficial effect on intestinal fibrosis associated with chronic colitis.

#### UC/PL-MSC-CM inhibits TGF- $\beta$ 1-induced ECM and $\alpha$ -SMA expression in human intestinal myofibroblasts

HIMFs were co-cultured with UC/PL-MSC-CM and simultaneously stimulated with TGF- $\beta$ 1 to evaluate the anti-fibrotic effects of human UC/PL-MSC-CM on myofibroblasts. TGF- $\beta$ 1 significantly increased mRNA expression of collagen1A1 (*COL1A1*), FN (*FNI*), and  $\alpha$ -SMA (*ACTA2*) in HIMFs. In contrast, co-culture with UC/PL-MSC-CM significantly inhibited this effect in a dose-dependent manner (Fig. 4A, Additional file 1: Fig. S2 and Additional file 2). Notably, the comparison between UC-MSC-CM and PL-MSC-CM treatments revealed no significant difference in the expression levels of *ACTA2* mRNA. However, a more pronounced reduction in the expression of *COL1A1* and *FNI* mRNA was observed with the application of UC-MSC-CM. At the protein level, treatment with UC-MSC-CM resulted in a significant reduction of the TGF- $\beta$ 1-induced increase in Procol1A1 protein expression. In contrast, while PL-MSC-CM treatment also displayed a trend towards decreased Procol1A1 protein expression, this reduction did not reach statistical significance (Fig. 4B, C; Additional file 1: Fig. S3). UC/PL-MSC-CM also significantly reduced the TGF- $\beta$ 1-induced upregulation of FN and  $\alpha$ -SMA protein expression. Contrary to the trends observed at the mRNA expression levels, the reduction in Procol1A1 and FN protein expression did not exhibit a statistically significant difference between the UC-MSC-CM and PL-MSC-CM treatments. However, the reduction in  $\alpha$ -SMA expression was significantly more pronounced in the UC-MSC-CM treatment group. In addition, the UC/PL-MSC-CM treatment significantly attenuated the Smad2 phosphorylation induced by TGF- $\beta$ 1 (Fig. 4B, C). This suggests that the anti-fibrogenic effects of UC/PL-MSC-CM may be mediated through Smad-dependent pathways.

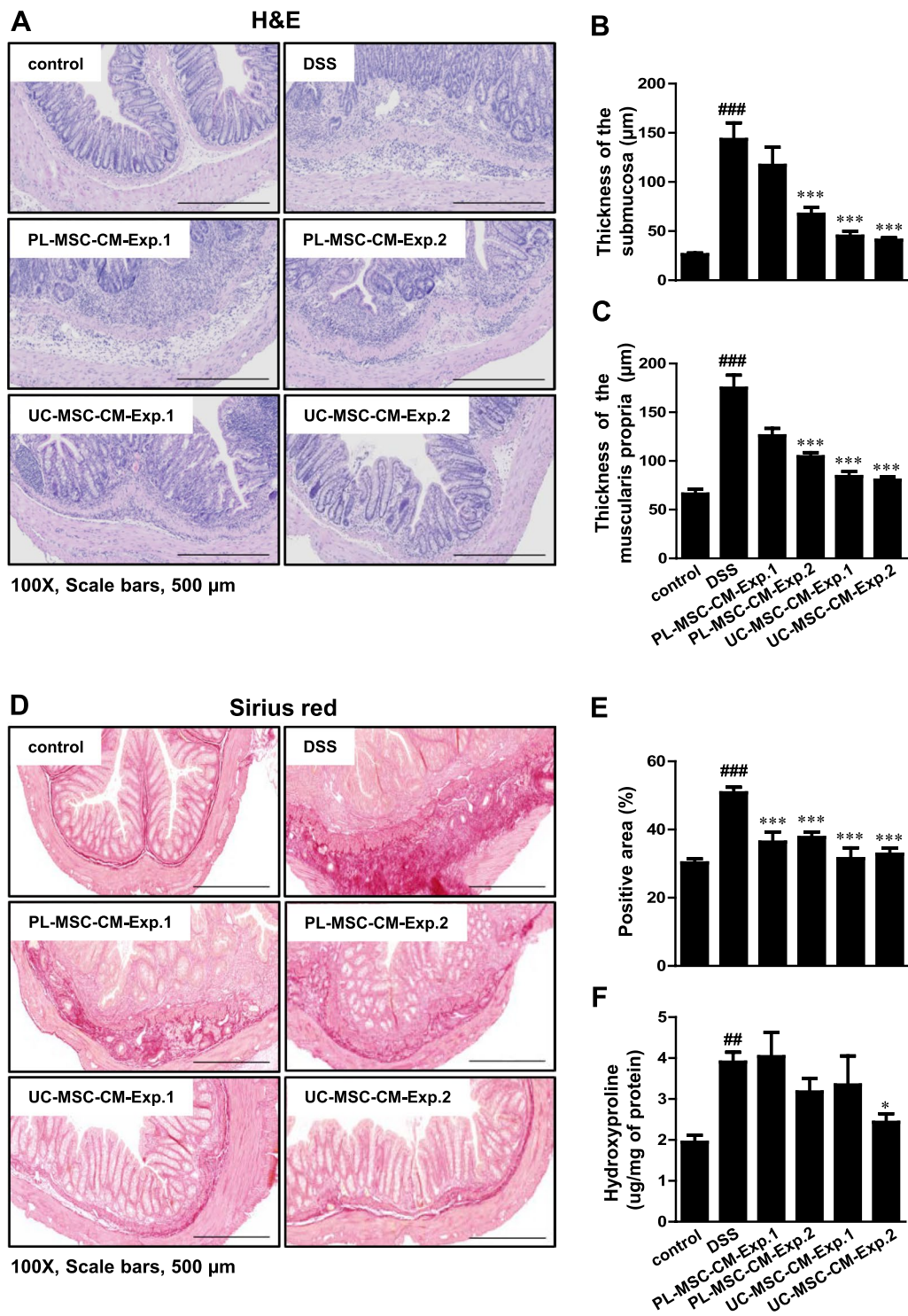


**Fig. 2** UC/PL-MSC-CM ameliorates inflammation-associated intestinal fibrosis in chronic DSS-induced colitis. **A** Representative hematoxylin and eosin [H&E] staining of colon sections. **B** Submucosal thickness ( $\mu\text{m}$ ). **C** Muscularis propria thickness ( $\mu\text{m}$ ). **D** Representative Sirius red staining of colon sections. **E** Positive area (%) in Sirius red staining. **F** Hydroxyproline concentration ( $\mu\text{g}/\text{mg}$  of protein). Data are expressed as means  $\pm$  SEM ( $n = 10\text{--}15$  in each group).  $^{##}P < .01$  and  $^{###}P < .001$  versus the control group;  $^{*}P < .05$  and  $^{***}P < .001$  versus the DSS group (ANOVA w/ Tukey). Scale bars, 500  $\mu\text{m}$ ; original magnification,  $\times 100$  (**A**, **D**)

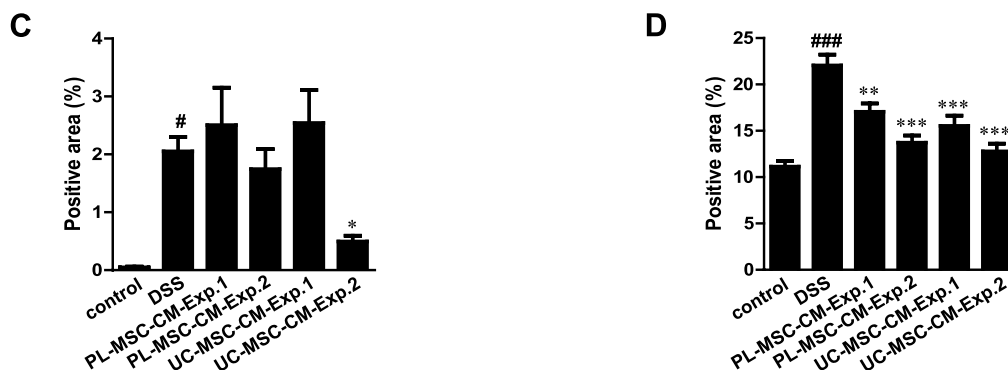
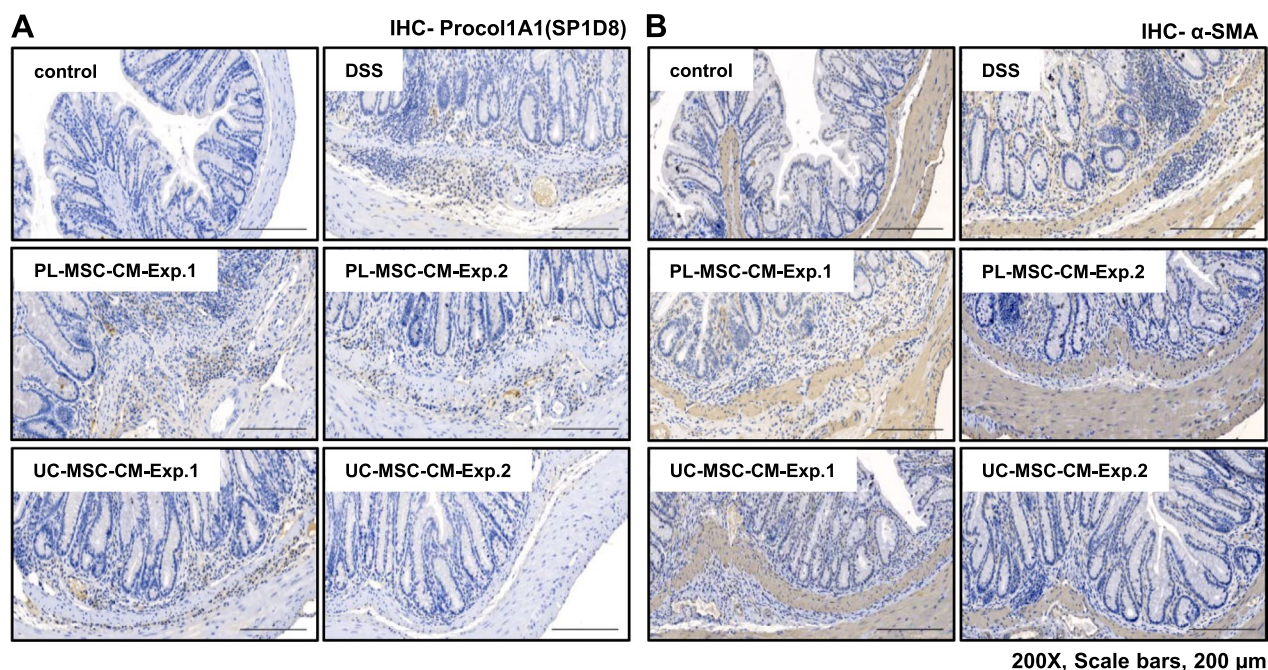


**Fig. 3** Immunohistochemical (IHC) staining of Procol1A1 and  $\alpha$ -SMA. **A** Representative IHC staining of Procol1A1. **B** Representative IHC staining of  $\alpha$ -SMA. **C** Procol1A1 quantification by IHC staining of the colon. **D**  $\alpha$ -SMA quantification by IHC staining of the colon. Data are presented as mean  $\pm$  SEM. <sup>#</sup> $P < .05$  and <sup>###</sup> $P < .001$  versus the control group. <sup>\*</sup> $P < .05$ , <sup>\*\*</sup> $P < .01$ , and <sup>\*\*\*</sup> $P < .001$  versus the DSS group (ANOVA w/ Tukey). Scale bars, 200  $\mu$ m; original magnification,  $\times 200$  (A, B)

Immunostaining of Procol1A1 and  $\alpha$ -SMA in HIMFs treated with TGF- $\beta$ 1 revealed a significant increase in Procol1A1 staining and the presence of well-organized, intensely stained actin stress fibers (Fig. 5A, B). However, treatment with UC/PL-MSC-CM resulted in a reduction of Procol1A1 staining and produced a diffuse, less intense  $\alpha$ -SMA staining, similar to that observed in control samples. These findings suggest that both UC- and PL-MSC-CM are capable of effectively inhibiting the fibrogenic activation of HIMFs induced by TGF- $\beta$ 1, as evidenced by the downregulation of ECM components and  $\alpha$ -SMA at both the mRNA and protein levels.

#### UC/PL-MSC-CM inhibits the Rho/MRTF/SRF signaling in human intestinal myofibroblasts.

We investigated the role of the Rho/MRTF/SRF signaling pathway in the anti-fibrotic effects of UC/PL-MSC-CM. UC/PL-MSC-CM significantly reduced *MRTFA* mRNA expression induced by TGF- $\beta$ 1 in HIMFs, while only UC-MSC-CM significantly reduced *SRF* mRNA expression (Fig. 6A). We also examined the expression of upstream signaling molecules, including *RHOA*, *ROCK1*, and *ROCK2*, which have been found to be important in fibrosis development in most organs [37]. The mRNA expression of *RHOA* and *ROCK1* induced by TGF- $\beta$ 1 in HIMFs was significantly reduced by co-culture

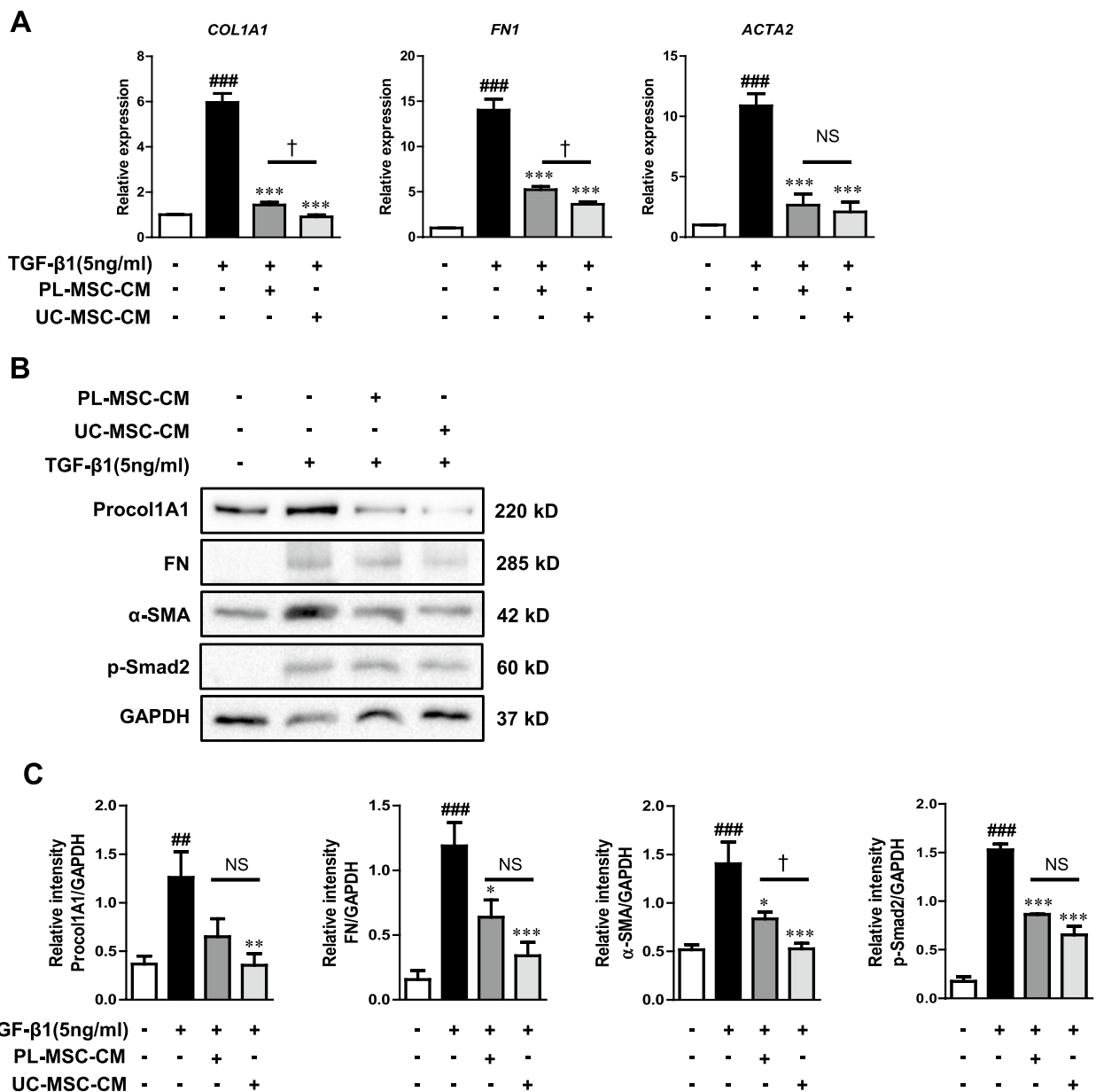


**Fig. 4** Co-culture with UC/PL-MSC-CM inhibits TGF-β1-induced fibrogenic activation of HIMFs. HIMFs were treated with TGF-β1 (5 ng/mL) and co-cultured with or without UC/PL-MSC-CM. **A** RT-qPCR analysis of the relative mRNA expression of collagen1A1 (*COL1A1*), fibronectin (*FN1*), and α-smooth muscle actin (*ACTA2*). The data were normalized to GAPDH expression and expressed as relative values compared to the control (n = 3). **B** Representative Western blots show the protein expression of procollagen1A1 (Procol1A1), fibronectin (FN), α-smooth muscle actin (α-SMA), and phosphorylated Smad2 (p-Smad2) with GAPDH as a loading control. **C** Quantitation of Procol1A1, FN, α-SMA, and p-Smad2 from Western blot analyses (n = 4). Data are expressed as means ± SEM. ##*P* < .01 and ###*P* < .001 versus the control; \**P* < .05, \*\**P* < .01, and \*\*\**P* < .001 versus the TGF-β1 treatment only (ANOVA w/ Tukey); †*P* < .05 compared between PL-MSC-CM and UC-MSC-CM (Mann-Whitney U test). NS, not significant. Full-length blots are presented in Additional file 1: Fig. S3

with UC/PL-MSC-CM, with no significant difference observed between the UC-MSC-CM and PL-MSC-CM. In addition, the expression level of *ROCK2* mRNA was significantly reduced in the co-culture treated with UC/PL-MSC-CM compared to the treatment with

TGF-β1 alone. Contrary to *ROCK1*, there was a decrease in *ROCK2* mRNA expression in response to TGF-β1 treatment (Fig. 6A).

At the protein level, treatment with UC-MSC-CM resulted in a significant reduction in the expression of

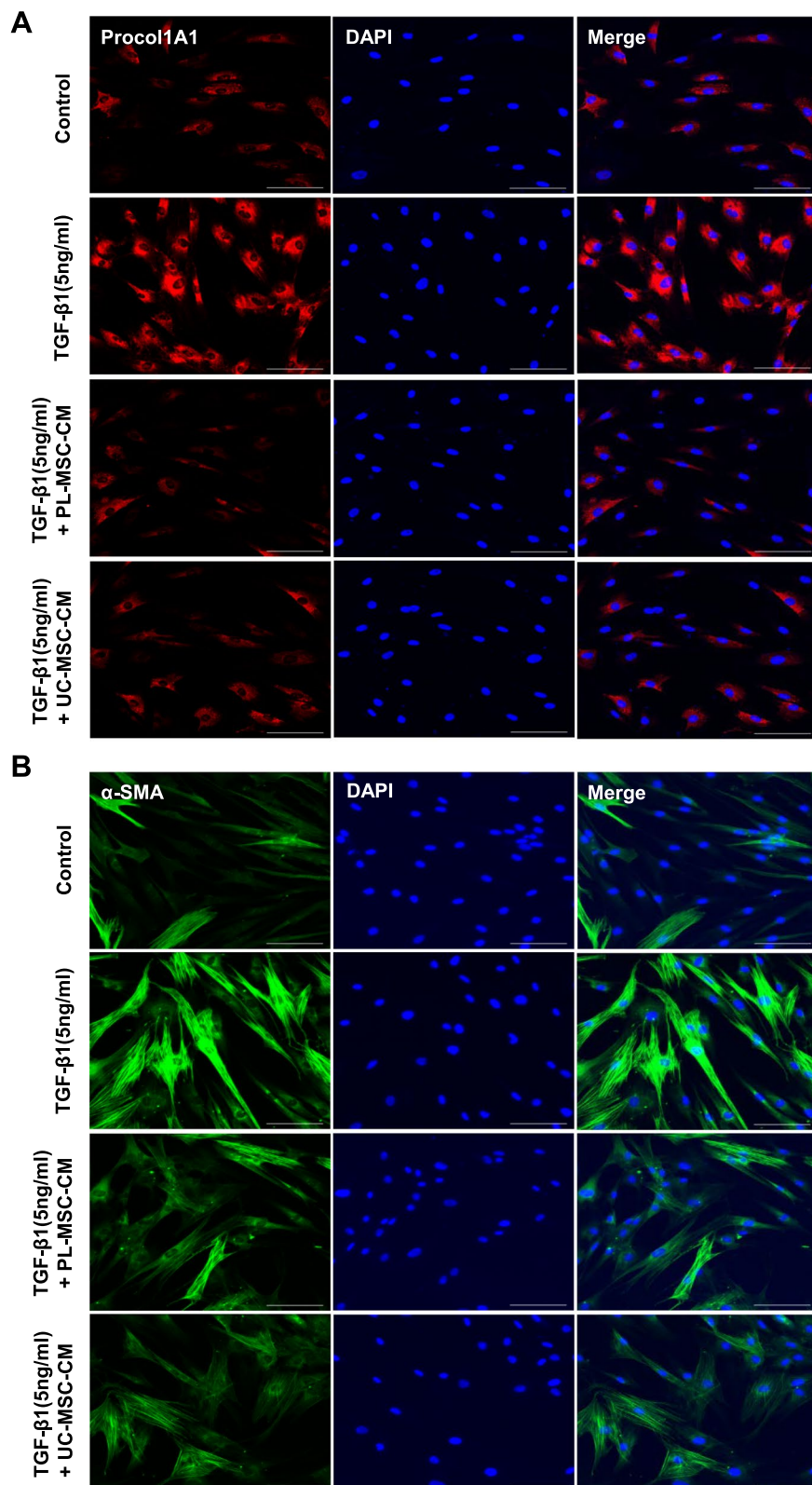


**Fig. 5** Co-culture with UC/PL-MSC-CM inhibits TGF-β1-induced Procol1A1 and α-SMA expression in HIMFs. **A–B** HIMFs were treated with TGF-β1 (5 ng/mL) and co-cultured with or without UC/PL-MSC-CM and then stained with Procol1A1 (**A**) and α-SMA (**B**) antibodies and counterstained with DAPI. Scale bars, 100 μm; original magnification, ×200

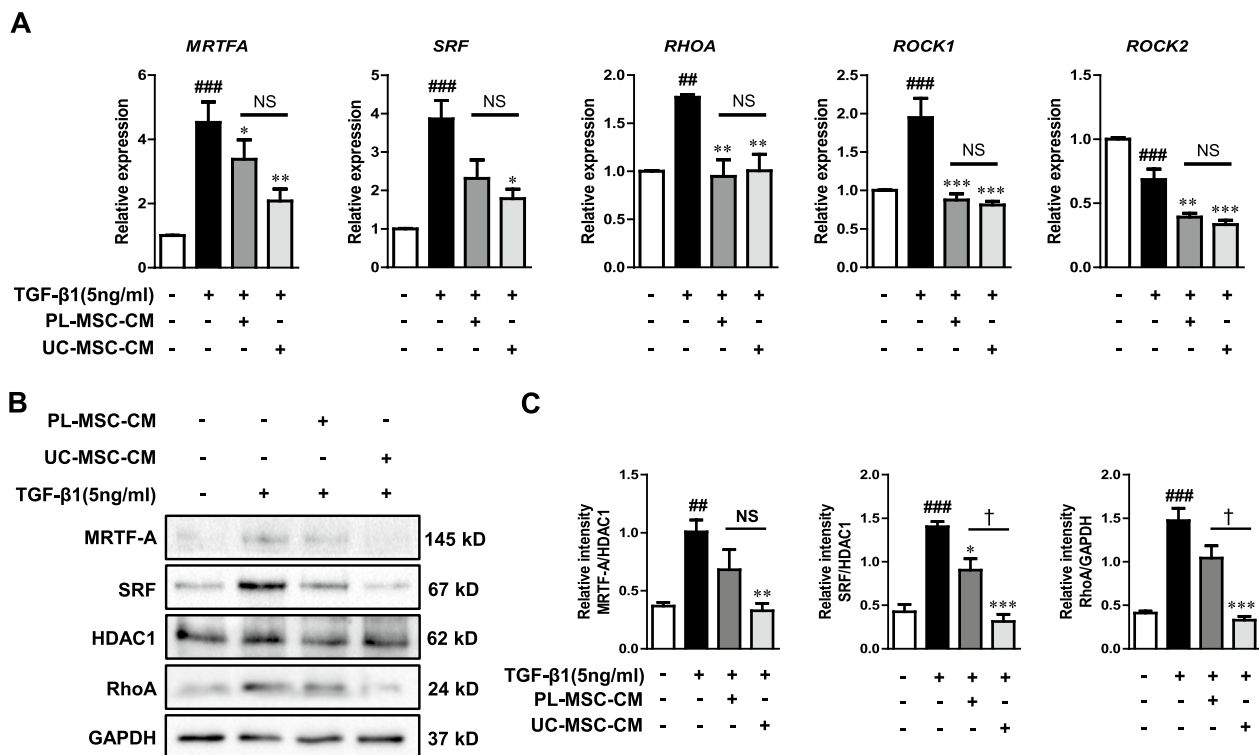


**Fig. 6** UC/PL-MSC-CM inhibits Rho/MRTF/SRF signaling in HIMFs. HIMFs were treated with TGF-β1 (5 ng/mL) and co-cultured with or without UC/PL-MSC-CM. **A** RT-qPCR analysis of the relative mRNA expression of *MRTFA*, *SRF*, *RHOA*, *ROCK1*, and *ROCK2*. The data were normalized to GAPDH expression and expressed as relative values compared to the control ( $n=3$ ). **B** Representative western blots show the protein expression of MRTF-A, SRF, and RhoA (MRTF-A and SRF from the nuclear extracts with HDAC1 as a loading control and RhoA from the cytosolic extracts with GAPDH as a loading control). **C** Quantitation of MRTF-A, SRF, and RhoA from western blot analyses ( $n=3$ ). Data are expressed as the means  $\pm$  SEM. ## $P < .01$  and ### $P < .001$  versus the control; \* $P < .05$ , \*\* $P < .01$  and \*\*\* $P < .001$  versus the TGF-β1 treatment only (ANOVA w/ Tukey); † $P < .05$  compared between PL-MSC-CM and UC-MSC-CM (Mann-Whitney U test). NS, not significant. Full-length blots are presented in Additional file 1: Fig. S4

MRTF-A and SRF in nuclear extracts, as well as RhoA in cytosolic extracts. All of these proteins had previously been stimulated by TGF-β1 (Fig. 6B, C; Additional file 1: Fig. S4). Treatment with PL-MSC-CM led to a significant reduction in SRF expression, while also showing a downward trend in the expression levels of MRTF-A and RhoA. Furthermore, the extent of reduction in SRF and RhoA expressions was significantly more pronounced in the UC-MSC-CM treatment compared to the PL-MSC-CM (Fig. 6B, C; Additional file 1: Fig. S4).

To further investigate the mechanisms underlying the anti-fibrotic properties of UC/PL-MSC-CM, we explored the potential role of MRTF-A nuclear localization inhibition in this anti-fibrotic process. This involved a specific quantification of the nuclear-to-cytoplasmic signal ratio in MRTF-A immunocytochemistry. The application of UC/PL-MSC-CM was associated with a significant decrease in MRTF-A nuclear localization (Fig. 7A, B). These results suggest that UC/PL-MSC-CM may exert its anti-fibrotic effects by inhibiting Rho/MRTF/SRF signaling pathways in HIMFs.

## Discussion

Our in vivo study revealed that UC/PL-MSC-CM alleviated inflammation-associated intestinal fibrosis in chronic DSS-induced colitis. Through the downregulation of Procol1A1 and  $\alpha$ -SMA, UC/PL-MSC-CM treatment prevented the development of intestinal fibrosis in chronic colitis produced by repeated cycles of DSS exposure. The anti-fibrotic effect was more significant in the UC-MSC-CM group or in the early-phase treatment model (Exp. 2), where the CM was administered twice weekly starting from day 29. Furthermore, our in vitro results showed that UC/PL-MSC-CM inhibits TGF-β1-induced ECM (Procol1A1 and FN) synthesis and  $\alpha$ -SMA formation in HIMFs by blocking Rho/MRTF/SRF signaling. These findings suggest that UC/PL-MSC-CM is a promising choice for stem cell-based therapy of intestinal fibrosis.

MSCs exhibit anti-fibrotic properties, suggesting that they may have therapeutic implications for fibrotic diseases [38–41]. Although research in this area is still limited, there is evidence that MSCs, including UC/

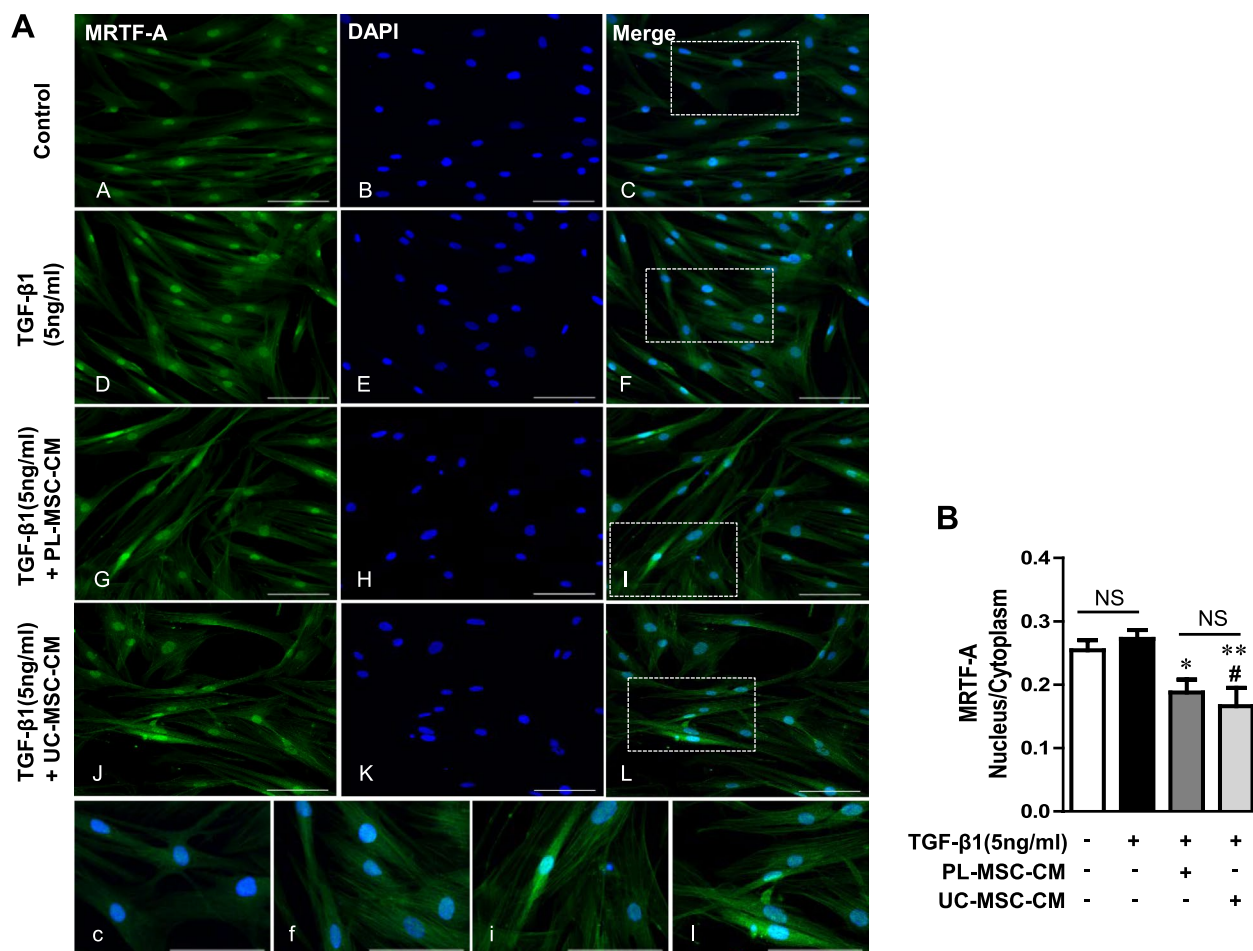


**Fig. 7** UC/PL-MSC-CM inhibits MRTF-A nuclear localization in HIMFs. HIMFs were treated with TGF-β1 (5 ng/mL), co-cultured with or without UC/PL-MSC-CM, stained with MRTF-A antibodies, and counterstained with DAPI. **A** (A–C) no treatment; (D–F) treatment with TGF-β1; (G–I) treatment with TGF-β1 and PL-MSC-CM; (J–L) treatment with TGF-β1 and UC-MSC-CM; (c, f, i, l) Enlarged images of the region (within the white box of C, F, I, and L, each). **B** The nuclear-to-cytoplasmic ratio of MRTF-A was determined for each condition as described in the "Methods" section. Data are expressed as means ± SEM. # $P < .05$  versus the control; \* $P < .05$  and \*\* $P < .01$  versus the TGF-β1 treatment only (ANOVA w/ Tukey). NS, not significant (Mann–Whitney U test); Scale bars, 100 μm; original magnification, ×200 (**A**)

PL-MSCs, are promising for the prevention and treatment of fibrogenesis, particularly in intestinal fibrosis [23, 42]. However, various issues must be addressed, such as MSC heterogeneity, short lifespan, and potential tumorigenic risks, especially when used in high doses or after genetic modification [43–45]. In terms of therapy, MSCs primarily operate through paracrine signaling, releasing a mixture of soluble factors and EVs into their CM. The CM, which combines these elements, offers advantages over whole MSCs, including reduced risks of tumorigenicity and immunological issues and ease of storage [46–48]. Furthermore, CM production is more cost-effective and efficient than EV isolation; CM benefits from high concentrations of soluble factors and EVs, particularly from adipose-derived MSCs [49]. Studies have

shown that MSC CM and EVs contain anti-fibrogenic agents, like HGF, TGF-β3, IL-10, MFGE-8, miR-27b, and miR-223-3p, which are capable of blocking the TGF-β1/Smad2/3 signaling pathway and thereby inhibiting the transition of fibroblasts to myofibroblasts [31, 32, 50–55]. Hence, MSC-CM has emerged as a potentially useful therapeutic product.

Our in vivo study demonstrated that UC/PL-MSC-CM ameliorates intestinal fibrosis, as evidenced by reductions of collagen and α-SMA deposition based on measurements of the thickness of the submucosa and muscularis propria, Sirius red staining, hydroxyproline quantification, and Procol1A1 and α-SMA immunohistochemistry. Few studies have evaluated the MSC-CM in animal models of intestinal fibrosis. The effect of MSCs engineered to

overexpress hypoxia-inducible factor 1-alpha and telomerase (MSC-T-HIF) conditioned with pro-inflammatory stimuli to release EVs (EVMSC-T-HIFC) on the fibrosis and inflammatory response of activated endothelium was examined in a recent study investigating experimental CD [56]. EVMSC-T-HIFC administration to mice with acute TNBS-induced colitis accelerated mucosal healing, reduced inflammation, and alleviated intestinal fibrosis. A recent study in 2023 has shed light on the therapeutic potential of human UC MSC-derived exosomes (hucMSC-Ex) in the context of IBD-associated intestinal fibrosis. In animal models, hucMSC-Ex reduced inflammation-related fibrosis, inhibited TGF- $\beta$ -induced proliferation, migration, and activation of human intestinal fibroblasts, and decreased ERK phosphorylation, a key process in IBD-associated fibrosis [57]. Another study conducted in 2023 has revealed that the intratracheal application of MSC-EVs plays a pivotal role in the amelioration of established pulmonary fibrosis; this therapeutic effect can primarily be attributed to the transfer of specific microRNAs encapsulated within MSC-EVs [58]. Administration of the MSC culture supernatant significantly reduced the degree of luminal stricture in the rectum and mitigated myofibroblast activation and hypertrophy of the muscularis propria in pigs [59]. Various challenges remain in the field of MSC-based cell-free therapies for intestinal fibrosis, including an insufficient understanding of the MSC secretome and its intercellular interactions as well as the need to optimize the administration of MSC-derived components in terms of dosage, timing, and delivery methods.

MSC-EVs/exosomes exhibit the capacity to migrate to inflamed tissues, where they effectively interact with and modulate immune cells, actively regulating immune responses and exerting anti-inflammatory effects [60, 61]. In our study, we did not conduct live cell tracing to evaluate the migration of MSC-CM to the fibrotic area. Nevertheless, prior research provides some insights that might be pertinent to our findings. For example, a study published in 2015 demonstrated that intraperitoneally injected exosomes migrate to several organs, including the liver, lung, spleen, pancreas, and GI tract [62]. Of particular note in the context of the GI tract, exosome accumulation was significantly higher after intraperitoneal injection than after intravenous injection. Furthermore, the quantity of exosomes in the GI tract was comparable to that in the liver. These findings suggest that the intraperitoneal administration of exosomes is a promising therapeutic strategy for GI tract diseases [63]. A plausible interpretation of these findings is that lymphatic vessels lack a basement membrane, resulting in considerably greater permeability, enabling the diffusion of large molecules. Building upon this premise, peritoneally infused

exosomes could be readily absorbed by mesenteric or peritoneal lymphatics. Following uptake, these exosomes have the potential to migrate to various organs, including the GI tract [64].

Furthermore, intraperitoneally injected MSC-CM may induce anti-inflammatory and anti-fibrotic effects within the mesenteric fat. Accumulating evidence suggests that there is a connection between changes in the mesenteric fat and CD [65]. Intestinal barrier dysfunction and transmural inflammation may induce bacterial translocation to the surrounding mesenteric adipose tissue, which subsequently leads to adipocyte hypertrophy. The hypertrophic adipocytes release pro-inflammatory mediators, which can activate the infiltration of M1 macrophages and Th1 and Th17 cells into mesenteric fat [66, 67]. This process may contribute to the development of hypertrophic mesenteric fat wrapping around the inflamed intestine, known as “creeping fat,” which is pathognomonic of CD [65]. The creeping fat in CD is associated with intestinal fibrosis by releasing broad spectrum of profibrotic mediators [68, 69]. MSC-CM contains a range of soluble anti-inflammatory factors, such as IL-10 and TGF- $\beta$ . Upon intraperitoneal injection, these soluble factors can reach the mesenteric fat and may inhibit the activity of pro-fibrotic cells, such as M1 macrophages and Th1 and Th17 cells, within the mesenteric fat. The observed anti-fibrotic potential of intraperitoneally injected MSC-CM could be attributed to its influence on both innate and adaptive immune cells. This hypothesis is supported by a study of a DSS-induced colitis model, where UC-MSC-CM facilitated the polarization of M1 macrophages into an M2 phenotype. This shift was associated with a decrease in pro-fibrotic cytokines (IL-1 $\beta$ , MCP-1, TIMP-1, and IL-17) and an increase in the anti-fibrotic IL-10 in the colon or peritoneum [70]. Complementing these findings, Heidari et al. reported that UC-MSC exosomes prompt a similar immunomodulatory effect in a mouse model of DSS-induced colitis. They observed a Th1/Th17 polarization of regulatory T cells, leading to the reduced expression of pro-fibrotic mediators (TNF $\alpha$ , IL-17) and enhanced expression of the anti-fibrotic mediator IL-10 in mesenteric lymph nodes [71].

Additional file 1: Fig. S2 summarizes the mRNA expression levels of other fibrosis-related genes. In Exp. 2, the proinflammatory and profibrotic cytokine *Tnfa* was significantly reduced in the colon tissues of UC-MSC-CM-treated mice, consistent with the findings of previous studies, indicating that MSC-CM/EVs suppress TNF- $\alpha$  expression in a DSS colitis model [72–74]. Furthermore, in Exp. 2, mRNA expression levels of *Acta2*, *Tgfb1*, *Mmp9*, and *Timp1* were lower after the injection of UC-MSC-CM than in the DSS alone group; however, these differences were not statistically significant. This

finding points to ECM remodeling with a bias toward anti-fibrogenic processes in the colon. In contrast to TGF- $\beta$ 1 and TIMP-1, which act as fibrogenic molecules in intestinal fibrosis, MMP-9 is generally thought to have an anti-fibrogenic effect due to its collagen proteolytic activity. However, it can also induce fibrogenesis by releasing or activating various pro-fibrotic molecules sequestered in the ECM by proteolytic degradation and mediating epithelial-mesenchymal transition, a process in which epithelial cells undergo phenotypic metamorphosis into myofibroblasts [75]. In addition, other studies have shown that MSCs reduce intestinal or renal fibrosis by decreasing MMP-9 expression or activity [42, 75, 76].

We investigated the anti-fibrotic effects of UC/PL-MSC-CM in a late-phase treatment model (Exp. 1), where UC/PL-MSC-CM was injected from Day 50, and an early-phase treatment model (Exp. 2), where UC/PL-MSC-CM was injected from Day 29. In Exp. 2, UC-MSC-CM showed more significant anti-fibrotic effects based on relative weight (%), colon weight/length, collagen quantification by a hydroxyproline assay, and Procol1A1-positive area. In Exp. 2, PL-MSC-CM also showed more effective anti-fibrotic effects based on measurements of the colon length and thickness of the submucosa/muscularis propria. Overall, UC/PL-MSC-CM treatment was more effective in curing fibrosis in the early phase of chronic DSS-induced intestinal fibrosis than in the late phase. These findings are consistent with those of previous studies revealing that anti-fibrotic intervention is more effective when initiated early in the course of the disease. Previously, early eradication of the fibrotic stimulus suppressed intestinal fibrosis, while late eradication did not prevent fibrotic progression [3]. Another study has shown that an anti-fibrotic molecule administered prophylactically is highly effective in slowing the progression of intestinal fibrosis, while administration during the late phase of fibrosis is less effective in clearing fibrosis [77]. Overall, our findings suggest that early UC/PL-MSC-CM treatment may be more effective than late treatment during intestinal fibrosis.

Co-culture with the UC/PL-MSC-CM significantly inhibited TGF- $\beta$ 1-mediated fibrogenesis in the HIMFs, as revealed by decreased ECM (Procol1A1, FN) and contractile protein ( $\alpha$ -SMA) expression, along with a decrease in Smad2 phosphorylation. Several studies have shown that the UC/PL-MSC-CM inhibits fibroblast differentiation into myofibroblasts and reduces ECM and  $\alpha$ -SMA expression in myofibroblasts [78, 79]. In addition, the discovery of reduced Smad2 phosphorylation in response to TGF- $\beta$ 1 treatment with the UC/PL-MSC-CM suggests that the anti-fibrogenic effects may occur via Smad-dependent mechanisms. UC-MSCs, but not PL-MSCs, decrease the TGF- $\beta$ 1-induced phosphorylation

of Smad2 and Smad3 [23]. In addition, UC-MSC-derived exosomes suppress Smad2 activation and reduce TGF- $\beta$ -induced  $\alpha$ -SMA expression in skin fibroblasts [80].

In this study, we compared the anti-fibrotic effects of MSC-CM derived from two different sources, the UC and PL. Immunomodulatory effects are greater for UC-MSCs than for PL-MSCs. This is because UC-MSCs have higher expression of immunomodulatory factors, such as TGF- $\beta$ , IL-10, and IDO (indoleamine 2,3-dioxygenase), all of which play important roles in immune regulation and inflammation suppression [81–84]. Additionally, a comparison of MSCs from various sources has shown that UC-MSCs exhibit the most significant immunosuppressive effects and the highest proliferative and differentiation potential [85]. Previously, we found that UC-MSCs exhibit pronounced anti-fibrotic activities in HIMFs [23]. Similarly, compared with the effects of PL-MSC-CM, UC-MSC-CM demonstrated more potent inhibitory effects in the chronic DSS-induced intestinal fibrosis model as well as on TGF-1-induced Procol1A1, FN, and  $\alpha$ -SMA expression in HIMFs and the protein expression of MRTF-A, SRF, and RhoA. Thus, these findings suggest that UC-MSC-CM has more potent anti-fibrotic activity than that of PL-MSC-CM.

The Rho/ROCK/Actin/MRTF/SRF signaling axis, a Smad-independent pathway, is a key pathway involved in multiple types of solid organ fibrosis, including intestinal fibrosis [86–89]. RhoA, a GTPase from the Rho family, promotes G-actin integration into F-actin. Furthermore, RhoA-mediated ROCK activation inhibits F-actin depolymerization [90]. F-actin polymerization results in the release of G-actin-bound MRTF-A, which translocates to the nucleus and interacts with SRF, inducing the expression of fibrogenic genes, such as collagen 1A1 and  $\alpha$ -SMA [9, 11]. Recent studies have shed light on the role of Rho/ROCK/Actin/MRTF/SRF signaling in intestinal fibrosis [9, 91, 92]. Our previous study has revealed that the anti-fibrogenic effects of UC/PL-MSCs are mediated via the Rho/MRTF/SRF signal pathway in HIMFs [23]. In this study, co-culture with UC/PL-MSC-CM suppressed ECM and  $\alpha$ -SMA expression in HIMFs by attenuating TGF- $\beta$ 1-induced MRTF-A and SRF expression and inhibiting MRTF-A nuclear translocation. These findings indicate that the anti-fibrotic effects of UC/PL-MSC-CM may be mediated via a mechanism involving the MRTF/SRF pathway. We assessed RhoA, ROCK1, and ROCK2 expression in HIMFs to determine whether UC/PL-MSC-CM affects factors upstream of the MRTF/SRF pathway. UC/PL-MSC-CM reduced MRTF-A and SRF expression, while suppressing the expression of RhoA, ROCK1, and ROCK2. The Rho/ROCK signaling pathway is critical in MRTF/SRF transcriptional activation [11]. These findings imply that the UC/PL-MSC-CM

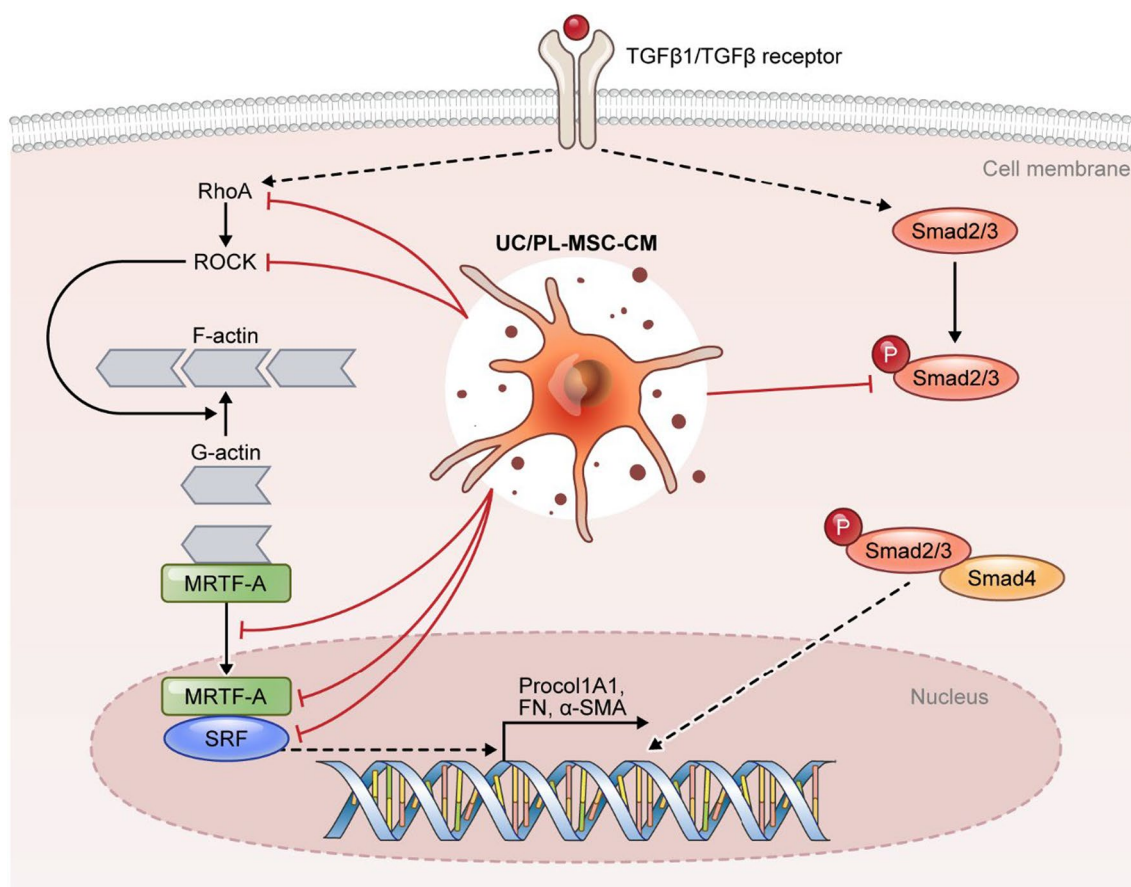


**Fig. 8** Model of the proposed mechanism of action of UC/PL-MSC-CM on TGF-β1-induced fibrogenic activation in HIMFs. TGF-β1 stimulates the expression of Procol1A1, FN, and α-SMA via the activation of the MRTF-A/SRF signaling and Smad2/3. UC/PL-MSC-CM counteract TGF-β1-induced fibrogenic responses by inhibiting the RhoA/MRTF-A/SRF signaling and Smad2/3 pathways

exerts an anti-fibrotic effect by modulating the upstream TGF-β pathway, resulting in a broader impact beyond the selective inhibition of MRTF/SRF and interfering with the Rho/ROCK pathway.

**Conclusions**

In this study, we observed that human UC/PL-MSC-CM exhibited anti-fibrotic properties in a murine model of intestinal fibrosis. The primary mechanisms underpinning these effects appear to be the suppression of collagen synthesis and the downregulation of α-SMA expression. Furthermore, UC/PL-MSC-CM showed a remarkable capability in mitigating TGF-β1-induced fibrogenic activation in HIMFs through the inhibition of the Rho/MRTF/SRF signaling pathway, as depicted in Fig. 8. Notably, the anti-fibrogenic effect was more pronounced in the UC-MSC-CM treatment or when applied in the early-phase of the model. Consequently, UC/PL-MSC-CM may emerge as a novel therapeutic approach for intestinal fibrosis. Nevertheless, further studies are

essential to elucidate the precise mechanisms and identify the key anti-fibrotic constituents within MSC-CM, in order to confirm these findings and refine the therapeutic application of UC/PL-MSC-CM.

**Abbreviations**

HIMFs	Human primary intestinal myofibroblasts
DSS	Dextran sulfate sodium
IBD	Inflammatory bowel disease
CD	Crohn's disease
GI	Gastrointestinal
ECM	Extracellular matrix
α-SMA	α-Smooth muscle actin
TGF-β1	Transforming growth factor
G-actin	Promoting globular actin
F-actin	Filamentous actin
MRTF-A	Myocardin-related transcription factor A
SRF	Serum response factor
MSCs	Mesenchymal stem cells
UC/PL-MSCs	Umbilical cord and placenta-derived mesenchymal stem cells
CM	Conditioned medium
EVs	Extracellular vesicles
MMP	Matrix metalloproteinases
IL-10	Interleukin-10

HGF	Hepatocyte growth factor
miRNAs	MicroRNAs
$\alpha$ -MEM	$\alpha$ -modified minimal essential medium
FBS	Fetal bovine serum
FGF4	Fibroblast growth factor-4
FACS	Fluorescence-activated cell sorting
SEM	Standard error of the mean
FN	Fibronectin
hucMSC-Ex	Human UC MSC-derived exosomes

## Supplementary Information

The online version contains supplementary material available at <https://doi.org/10.1186/s13287-024-03678-4>.

**Additional file 1.** Supplementary figures.

**Additional file 2.** Supplementary methods and figure legends.

## Acknowledgements

We thank all members of our laboratory for their assistance.

## Author contributions

YJC, WRK, DHK, JHK, and JHY performed the experiments. YJC, JHK, and JHY analyzed the data. JHK and JHY designed the research. YJC and JHK drafted the manuscripts. YJC, JHK, and JHY edited and revised the manuscript. JHK and JHY performed a critical revision of the manuscript and supervised the study. All authors read and approved the final manuscript.

## Funding

This research was supported by the National Research Foundation of Korea (NRF) grant from the Korean government [The Ministry of Science and ICT; NRF-2020R1F1A1066323, NRF-2021R1F1A1061550, and NRF-2019R111A1A01061623]. The funding body played no role in the design of the study; the collection, analysis, and interpretation of data; or the writing of the manuscript.

## Availability of data and materials

All reported data have been obtained from experiments performed in the author's laboratory. The dataset generated during the present study is available upon reasonable request from the corresponding authors (Prof. Jee Hyun Kim or Prof. Jun Hwan Yoo).

## Declarations

### Ethical approval and consent to participate

This study adheres to the Declaration of Helsinki and was approved by Institutional Review Board of the CHA Bundang Medical Center, Korea (Title of the approved project: Anti-fibrogenic effect of PPAR- $\gamma$  agonists in activated human colonic myofibroblasts; Approval number: BD2014-195; Date of approval: 01/09/2015). Written informed consent for specimens was obtained from all participants. Title of the approved project: anti-fibrotic role of human umbilical cord/placenta-derived mesenchymal stem cell conditioned medium in intestinal fibrosis model. Name of the institutional approval committee or unit: The ethics committee at CHA University. Approval number: 210145. Date of approval: November 1, 2021. All animal experiments conform to the Animal Research: Reporting of In Vivo Experiments (ARRIVE) guidelines.

### Consent for publication

Not applicable.

### Competing interests

The authors declare that they have no competing interests.

### Author details

<sup>1</sup>Department of Gastroenterology, CHA Bundang Medical Center, CHA University School of Medicine, 59 Yatap-ro, Bundang-gu, Seongnam 13496, South Korea. <sup>2</sup>Institute of Basic Medical Sciences, CHA University School of Medicine,

Seongnam 13496, South Korea. <sup>3</sup>Department of Surgery, Gangnam Severance Hospital, Yonsei University College of Medicine, Seoul 06273, South Korea.

Received: 23 October 2023 Accepted: 21 February 2024

Published online: 07 March 2024

## References

- Baumgart DC, Carding SR. Inflammatory bowel disease: cause and immunobiology. *Lancet*. 2007;369:1627–40.
- Thia KT, Sandborn WJ, Harmsen WS, Zinsmeister AR, Loftus EV Jr. Risk factors associated with progression to intestinal complications of Crohn's disease in a population-based cohort. *Gastroenterology*. 2010;139:1147–55.
- Johnson LA, Luke A, Sauder K, Moons DS, Horowitz JC, Higgins PD. Intestinal fibrosis is reduced by early elimination of inflammation in a mouse model of IBD: impact of a "top-down" approach to intestinal fibrosis in mice. *Inflamm Bowel Dis*. 2012;18:460–71.
- Latella G, Di Gregorio J, Flati V, Rieder F, Lawrance IC. Mechanisms of initiation and progression of intestinal fibrosis in IBD. *Scan J Gastroenterol*. 2015;50:53–65.
- Gabbiani G. The myofibroblast in wound healing and fibrocontractive diseases. *J Pathol*. 2003;200:500–3.
- Hinz B. Tissue stiffness, latent TGF- $\beta$ 1 activation, and mechanical signal transduction: implications for the pathogenesis and treatment of fibrosis. *Curr Rheumatol Rep*. 2009;11:120–6.
- Koo JB, Nam M-O, Jung Y, Yoo J, Kim DH, Kim G, et al. Anti-fibrogenic effect of PPAR- $\gamma$  agonists in human intestinal myofibroblasts. *BMC Gastroenterol*. 2017;17:73.
- Biancheri P, Giuffrida P, Docena GH, MacDonald TT, Corazza GR, Di Sabatino A. The role of transforming growth factor (TGF)- $\beta$  in modulating the immune response and fibrogenesis in the gut. *Cytokine Growth Factor Rev*. 2014;25:45–55.
- Johnson LA, Rodansky ES, Haak AJ, Larsen SD, Neubig RR, Higgins PD. Novel Rho/MRTF/SRF inhibitors block matrix-stiffness and TGF- $\beta$ -induced fibrogenesis in human colonic myofibroblasts. *Inflamm Bowel Dis*. 2014;20:154–65.
- Derynck R, Zhang YE. Smad-dependent and Smad-independent pathways in TGF- $\beta$  family signalling. *Nature*. 2003;425:577–84.
- Small EM. The actin-MRTF-SRF gene regulatory axis and myofibroblast differentiation. *J Cardiovasc Transl Res*. 2012;5:794–804.
- Zhang Z, Lin H, Shi M, Xu R, Fu J, Lv J, et al. Human umbilical cord mesenchymal stem cells improve liver function and ascites in decompensated liver cirrhosis patients. *J Gastroenterol Hepatol*. 2012;27:112–20.
- Eom YW, Shim KY, Baik SK. Mesenchymal stem cell therapy for liver fibrosis. *Korean J Int Med*. 2015;30:580–9.
- Reinders ME, de Fijter JW, Roelofs H, Bajema IM, de Vries DK, Schaapherder AF, et al. Autologous bone marrow-derived mesenchymal stromal cells for the treatment of allograft rejection after renal transplantation: results of a phase I study. *Stem Cells Transl Med*. 2013;2:107–11.
- Karantalis V, Hare JM. Use of mesenchymal stem cells for therapy of cardiac disease. *Circ Res*. 2015;116:1413–30.
- Hare JM, Fishman JE, Gerstenblith G, DiFede Velazquez DL, Zambrano JP, Suncion VY, et al. Comparison of allogeneic vs autologous bone marrow-derived mesenchymal stem cells delivered by transendocardial injection in patients with ischemic cardiomyopathy: the POSEIDON randomized trial. *JAMA*. 2012;308:2369–79.
- Herrera MB, Bussolati B, Bruno S, Fonsato V, Romanazzi GM, Camussi G. Mesenchymal stem cells contribute to the renal repair of acute tubular epithelial injury. *Int J Mol Med*. 2004;14:1035–41.
- Kisseleva T, Uchinami H, Feirt N, Quintana-Bustamante O, Segovia JC, Schwabe RF, et al. Bone marrow-derived fibrocytes participate in pathogenesis of liver fibrosis. *J Hepatol*. 2006;45:429–38.
- Lee RH, Pulin AA, Seo MJ, Kota DJ, Ylostalo J, Larson BL, et al. Intravenous hMSCs improve myocardial infarction in mice because cells embolized in lung are activated to secrete the anti-inflammatory protein TSG-6. *Cell Stem Cell*. 2009;5:54–63.
- Lozito TP, Tuan RS. Mesenchymal stem cells inhibit both endogenous and exogenous MMPs via secreted TIMPs. *J Cell Physiol*. 2011;226:385–96.

21. Merino-González C, Zuñiga FA, Escudero C, Ormazabal V, Reyes C, Nova-Lamperti E, et al. Mesenchymal stem cell-derived extracellular vesicles promote angiogenesis: potential clinical application. *Front Physiol.* 2016;7:24.
22. Oh JY, Kim MK, Shin MS, Lee HJ, Ko JH, Wee WR, et al. The anti-inflammatory and anti-angiogenic role of mesenchymal stem cells in corneal wound healing following chemical injury. *Stem Cells.* 2008;26:1047–55.
23. Choi YJ, Koo JB, Kim HY, Seo JW, Lee EJ, Kim WR, et al. Umbilical cord/placenta-derived mesenchymal stem cells inhibit fibrogenic activation in human intestinal myofibroblasts via inhibition of myocardin-related transcription factor A. *Stem Cell Res Ther.* 2019;10:291.
24. Musiał-Wysocka A, Kot M, Majka M. The pros and cons of mesenchymal stem cell-based therapies. *Cell Transplant.* 2019;28:801–12.
25. Walczak P, Zhang J, Gilad AA, Kedziorek DA, Ruiz-Cabello J, Young RG, et al. Dual-modality monitoring of targeted intraarterial delivery of mesenchymal stem cells after transient ischemia. *Stroke.* 2008;39:1569–74.
26. Røslund GV, Svendsen A, Torsvik A, Sobala E, McCormack E, Immervoll H, et al. Long-term cultures of bone marrow-derived human mesenchymal stem cells frequently undergo spontaneous malignant transformation. *Cancer Res.* 2009;69:5331–9.
27. Kalinina N, Kharlampieva D, Loguinova M, Butenko I, Pobeguts O, Efimenko A, et al. Characterization of secretomes provides evidence for adipose-derived mesenchymal stromal cells subtypes. *Stem Cell Res Ther.* 2015;6:221.
28. Samad S, Akram K, Forsyth N, Spiteri M. Mesenchymal stem cell conditioned media (MSC-CM) suppress Wnt-3a and TGF- $\beta$ 1-induced myofibroblastic differentiation. *J Stem Cell Res Rev Rep.* 2014;1:1015.
29. Cahill EF, Kennelly H, Carty F, Mahon BP, English K. Hepatocyte growth factor is required for mesenchymal stromal cell protection against bleomycin-induced pulmonary fibrosis. *Stem Cells Transl Med.* 2016;5:1307–18.
30. Li Y, Zhang J, Shi J, Liu K, Wang X, Jia Y, et al. Exosomes derived from human adipose mesenchymal stem cells attenuate hypertrophic scar fibrosis by miR-192-5p/IL-17RA/Smad axis. *Stem Cell Res Ther.* 2021;12:221.
31. Li D, Zhang J, Liu Z, Gong Y, Zheng Z. Human umbilical cord mesenchymal stem cell-derived exosomal miR-27b attenuates subretinal fibrosis via suppressing epithelial–mesenchymal transition by targeting HOXC6. *Stem Cell Res Ther.* 2021;12:24.
32. Hou L, Zhu Z, Jiang F, Zhao J, Jia Q, Jiang Q, et al. Human umbilical cord mesenchymal stem cell-derived extracellular vesicles alleviated silica induced lung inflammation and fibrosis in mice via circPWV2A/miR-223–3p/NLRP3 axis. *Ecotoxicol Environ Saf.* 2023;251:114537.
33. Oh S-H, Choi C, Noh J-E, Lee N, Jeong Y-W, Jeon I, et al. Interleukin-1 receptor antagonist-mediated neuroprotection by umbilical cord-derived mesenchymal stromal cells following transplantation into a rodent stroke model. *Exp Mol Med.* 2018;50:1–12.
34. Kim MJ, Shin KS, Jeon JH, Lee DR, Shim SH, Kim JK, et al. Human choriionic-plate-derived mesenchymal stem cells and Wharton's jelly-derived mesenchymal stem cells: a comparative analysis of their potential as placenta-derived stem cells. *Cell Tissue Res.* 2011;346:53–64.
35. Kho AR, Kim OJ, Jeong JH, Yu JM, Kim HS, Choi BY, et al. Administration of placenta-derived mesenchymal stem cells counteracts a delayed anergic state following a transient induction of endogenous neurogenesis activity after global cerebral ischemia. *Brain Res.* 2018;1689:63–74.
36. Strong SA, Pizarro TT, Klein JS, Cominelli F, Fiocchi C. Proinflammatory cytokines differentially modulate their own expression in human intestinal mucosal mesenchymal cells. *Gastroenterology.* 1998;114:1244–56.
37. Nalkurthi C, Schroder WA, Melino M, Irvine KM, Nyuydzef M, Chen W, et al. ROCK2 inhibition attenuates profibrogenic immune cell function to reverse thioacetamide-induced liver fibrosis. *JHEP Rep.* 2022;4:100386.
38. Gao F, Chiu SM, Motan DA, Zhang Z, Chen L, Ji HL, et al. Mesenchymal stem cells and immunomodulation: current status and future prospects. *Cell Death Dis.* 2016;7(1):e2062.
39. Zhou Q, Rong C, Gu T, Li H, Wu L, Zhuansun X, et al. Mesenchymal stem cells improve liver fibrosis and protect hepatocytes by promoting microRNA-148a-5p-mediated inhibition of Notch signaling pathway. *Stem Cell Res Ther.* 2022;13:354.
40. Hu C, Zhao L, Duan J, Li L. Strategies to improve the efficiency of mesenchymal stem cell transplantation for reversal of liver fibrosis. *J Cell Mol Med.* 2019;23:1657–70.
41. Chen YS, Pelekanos RA, Ellis RL, Horne R, Wolvetang EJ, Fisk NM. Small molecule mesengenic induction of human induced pluripotent stem cells to generate mesenchymal stem/stromal cells. *Stem Cells Transl Med.* 2012;1:83–95.
42. Banerjee A, Bizzaro D, Burra P, Di Liddo R, Pathak S, Arcidiacono D, et al. Umbilical cord mesenchymal stem cells modulate dextran sulfate sodium induced acute colitis in immunodeficient mice. *Stem Cell Res Ther.* 2015;6:79.
43. Eiro N, Fraile M, González-Jubete A, González LO, Vizoso FJ. Mesenchymal (Stem) stromal cells based as new therapeutic alternative in inflammatory bowel disease: basic mechanisms, experimental and clinical evidence, and challenges. *Int J Mol Sci.* 2022;23:8905.
44. Sharma RR, Pollock K, Hubel A, McKenna D. Mesenchymal stem or stromal cells: a review of clinical applications and manufacturing practices. *Transfusion.* 2014;54:1418–37.
45. Uccelli A, Moretta L, Pistoia V. Mesenchymal stem cells in health and disease. *Nat Rev Immunol.* 2008;8:726–36.
46. Vizoso FJ, Eiro N, Cid S, Schneider J, Perez-Fernandez R. Mesenchymal stem cell secretome: toward cell-free therapeutic strategies in regenerative medicine. *Int J Mol Sci.* 2017;18:1852.
47. Osugi M, Katagiri W, Yoshimi R, Inukai T, Hibi H, Ueda M. Conditioned media from mesenchymal stem cells enhanced bone regeneration in rat calvarial bone defects. *Tissue Eng Part A.* 2012;18:1479–89.
48. Foo JB, Looi QH, Chong PP, Hassan NH, Yeo GEC, Ng CY, et al. Comparing the therapeutic potential of stem cells and their secretory products in regenerative medicine. *Stem Cells Int.* 2021;2021:2616807.
49. Giannasi C, Niada S, Magagnotti C, Ragni E, Andolfo A, Brini AT. Comparison of two ASC-derived therapeutics in an in vitro OA model: Secretome versus extracellular vesicles. *Stem Cell Res Ther.* 2020;11:521.
50. Mitchell R, Mellows B, Sheard J, Antonioli M, Kretz O, Chambers D, et al. Secretome of adipose-derived mesenchymal stem cells promotes skeletal muscle regeneration through synergistic action of extracellular vesicle cargo and soluble proteins. *Stem Cell Res Ther.* 2019;10:116.
51. Driscoll J, Patel T. The mesenchymal stem cell secretome as an acellular regenerative therapy for liver disease. *J Gastroenterol.* 2019;54:763–73.
52. Alfaifi M, Eom YW, Newsome PN, Baik SK. Mesenchymal stromal cell therapy for liver diseases. *J Hepatol.* 2018;68:1272–85.
53. Jang YJ, An SY, Kim J-H. Identification of MFG8 in mesenchymal stem cell secretome as an anti-fibrotic factor in liver fibrosis. *BMB Rep.* 2017;50:58–9.
54. Rong X, Liu J, Yao X, Jiang T, Wang Y, Xie F. Human bone marrow mesenchymal stem cells-derived exosomes alleviate liver fibrosis through the Wnt/ $\beta$ -catenin pathway. *Stem Cell Res Ther.* 2019;10:98.
55. Hu J, Chen Y, Huang Y, Su Y. Human umbilical cord mesenchymal stem cell-derived exosomes suppress dermal fibroblasts-myofibroblasts transition via inhibiting the TGF- $\beta$ 1/Smad 2/3 signaling pathway. *Exp Mol Pathol.* 2020;115:104468.
56. Gómez-Ferrer M, Amaro-Prellezo E, Dorronsoro A, Sánchez-Sánchez R, Vicente Á, Cosin-Roger J, et al. HIF-overexpression and pro-inflammatory priming in human mesenchymal stromal cells improves the healing properties of extracellular vesicles in experimental Crohn's Disease. *Int J Mol Sci.* 2021;22:11269.
57. Wang Y, Zhang Y, Lu B, Xi J, Ocansey DKW, Mao F, et al. HucMSC-Ex alleviates IBD-associated intestinal fibrosis by inhibiting ERK phosphorylation in intestinal fibroblasts. *Stem Cells Int.* 2023;2023:2828981.
58. Nataliya B, Mikhail A, Vladimir P, Olga G, Maksim V, Ivan Z, et al. Mesenchymal stromal cells facilitate resolution of pulmonary fibrosis by miR-29c and miR-129 intercellular transfer. *Exp Mol Med.* 2023;55:1399–412.
59. Tsuda M, Ohnishi S, Mizushima T, Hosono H, Yamahara K, Ishikawa M, et al. Preventive effect of mesenchymal stem cell culture supernatant on luminal stricture after endoscopic submucosal dissection in the rectum of pigs. *Endoscopy.* 2018;50:1001–16.
60. Rani S, Ryan AE, Griffin MD, Ritter T. Mesenchymal stem cell-derived extracellular vesicles: toward cell-free therapeutic applications. *Mol Ther.* 2015;23:812–23.
61. Phinney DG, Pittenger MF. Concise review: MSC-derived exosomes for cell-free therapy. *Stem Cells.* 2017;35:851–8.
62. Wiklander OP, Nordin JZ, O'Loughlin A, Gustafsson Y, Corso G, Mäger I, et al. Extracellular vesicle in vivo biodistribution is determined by cell source, route of administration and targeting. *J Extracell Vesicles.* 2015;4:26316.

63. Kang M, Jordan V, Blenkiron C, Chamley LW. Biodistribution of extracellular vesicles following administration into animals: a systematic review. *J Extracell Vesicles*. 2021;10:e12085.
64. Gupta D, Wiklander OP, Wood MJ, El-Andaloussi S. Biodistribution of therapeutic extracellular vesicles. *Extracell Vesicles Circ Nucleic Acids*. 2023;4:170–90.
65. Bilski J, Mazur-Bialy A, Wojcik D, Surmiak M, Magierowski M, Sliwowski Z, et al. Role of obesity, mesenteric adipose tissue, and adipokines in inflammatory bowel diseases. *Biomolecules*. 2019;9:780.
66. Suau R, Pardina E, Domènech E, Lorén V, Manyé J. The complex relationship between microbiota, immune response and creeping fat in Crohn's disease. *J Crohn's Colitis*. 2022;16:472–89.
67. Kim JH, Oh C-M, Yoo JH. Obesity and novel management of inflammatory bowel disease. *World J Gastroenterol*. 2023;29:1779–94.
68. Mao R, Doyon G, Gordon IO, Li J, Lin S, Wang J, et al. Activated intestinal muscle cells promote preadipocyte migration: a novel mechanism for creeping fat formation in Crohn's disease. *Gut*. 2022;71:55–67.
69. Mao R, Kurada S, Gordon IO, Baker ME, Gandhi N, McDonald C, et al. The mesenteric fat and intestinal muscle interface: creeping fat influencing stricture formation in Crohn's disease. *Inflamm Bowel Dis*. 2019;25:421–6.
70. Song JY, Kang HJ, Hong JS, Kim CJ, Shim JY, Lee CW, et al. Umbilical cord-derived mesenchymal stem cell extracts reduce colitis in mice by re-polarizing intestinal macrophages. *Sci Rep*. 2017;7:9412.
71. Heidari N, Abbasi-Kenarsari H, Namaki S, Baghaei K, Zali MR, Mirsanei Z, et al. Regulation of the Th17/Treg balance by human umbilical cord mesenchymal stem cell-derived exosomes protects against acute experimental colitis. *Exp Cell Res*. 2022;419:113296.
72. Legaki E, Roubelakis M, Theodoropoulos G, Lazaris A, Kollia A, Karamanolis G, et al. Therapeutic potential of secreted molecules derived from human amniotic fluid mesenchymal stem/stroma cells in a mice model of colitis. *Stem Cell Rev Rep*. 2016;12:604–12.
73. Mao F, Wu Y, Tang X, Kang J, Zhang B, Yan Y, et al. Exosomes derived from human umbilical cord mesenchymal stem cells relieve inflammatory bowel disease in mice. *Biomed Res Int*. 2017;2017:5356760.
74. Li Y, Altemus J, Lightner AL. Mesenchymal stem cells and acellular products attenuate murine induced colitis. *Stem Cell Res Ther*. 2020;11:515.
75. Matsui F, Babitz SA, Rhee A, Hile KL, Zhang H, Meldrum KK. Mesenchymal stem cells protect against obstruction-induced renal fibrosis by decreasing STAT3 activation and STAT3-dependent MMP-9 production. *Am J Physiol Renal Physiol*. 2017;312:F25–32.
76. Ye Y, Zhang X, Su D, Ren Y, Cheng F, Yao Y, et al. Therapeutic efficacy of human adipose mesenchymal stem cells in Crohn's colon fibrosis is improved by IFN- $\gamma$  and kynurenic acid priming through indoleamine 2,3-dioxygenase-1 signaling. *Stem Cell Res Ther*. 2022;13:465.
77. Lawrance IC, Wu F, Leite AZ, Willis J, West GA, Fiocchi C, et al. A murine model of chronic inflammation-induced intestinal fibrosis down-regulated by antisense NF- $\kappa$ B. *Gastroenterology*. 2003;125:1750–61.
78. Zhao Y, Yan Z, Liu Y, Zhang Y, Shi J, Li J, et al. Effectivity of mesenchymal stem cells for bleomycin-induced pulmonary fibrosis: a systematic review and implication for clinical application. *Stem Cell Res Ther*. 2021;12:470.
79. Yao Y, Huang J, Geng Y, Qian H, Wang F, Liu X, et al. Paracrine action of mesenchymal stem cells revealed by single cell gene profiling in infarcted murine hearts. *PLoS One*. 2015;10:e0129164.
80. Fang S, Xu C, Zhang Y, Xue C, Yang C, Bi H, et al. Umbilical cord-derived mesenchymal stem cell-derived exosomal microRNAs suppress myofibroblast differentiation by inhibiting the transforming growth factor- $\beta$ /SMAD2 pathway during wound healing. *Stem Cells Transl Med*. 2016;5:1425–39.
81. Zhang Q, Li Q, Zhu J, Guo H, Zhai Q, Li B, et al. Comparison of therapeutic effects of different mesenchymal stem cells on rheumatoid arthritis in mice. *PeerJ*. 2019;7:e7023.
82. Ma J, Wu J, Han L, Jiang X, Yan L, Hao J, et al. Comparative analysis of mesenchymal stem cells derived from amniotic membrane, umbilical cord, and chorionic plate under serum-free condition. *Stem Cell Res Ther*. 2019;10:19.
83. Chen G, Yue A, Ruan Z, Yin Y, Wang R, Ren Y, et al. Comparison of biological characteristics of mesenchymal stem cells derived from maternal-origin placenta and Wharton's jelly. *Stem Cell Res Ther*. 2015;6:1–7.
84. Li T, Xia M, Gao Y, Chen Y, Xu Y. Human umbilical cord mesenchymal stem cells: an overview of their potential in cell-based therapy. *Expert Opin Biol Ther*. 2015;15:1293–306.
85. Li X, Bai J, Ji X, Li R, Xuan Y, Wang Y. Comprehensive characterization of four different populations of human mesenchymal stem cells as regards their immune properties, proliferation and differentiation. *Int J Mol Med*. 2014;34:695–704.
86. Zhou N, Lee J-J, Stoll S, Ma B, Wiener R, Wang C, et al. Inhibition of SRF/myocardin reduces aortic stiffness by targeting vascular smooth muscle cell stiffening in hypertension. *Cardiovasc Res*. 2017;113:171–82.
87. Sisson TH, Ajayi IO, Subbotina N, Dodi AE, Rodansky ES, Chibucos LN, et al. Inhibition of myocardin-related transcription factor/serum response factor signaling decreases lung fibrosis and promotes mesenchymal cell apoptosis. *Am J Pathol*. 2015;185:969–86.
88. Xu H, Wu X, Qin H, Tian W, Chen J, Sun L, et al. Myocardin-related transcription factor A epigenetically regulates renal fibrosis in diabetic nephropathy. *J Am Soc Nephrol*. 2015;26:1648–60.
89. Haak AJ, Tsou PS, Amin MA, Ruth JH, Campbell P, Fox DA, et al. Targeting the myofibroblast genetic switch: inhibitors of myocardin-related transcription factor/serum response factor-regulated gene transcription prevent fibrosis in a murine model of skin injury. *J Pharmacol Exp Ther*. 2014;349:480–6.
90. Sotiropoulos A, Gineitis D, Copeland J, Treisman R. Signal-regulated activation of serum response factor is mediated by changes in actin dynamics. *Cell*. 1999;98:159–69.
91. Holvoet T, Devriese S, Castermans K, Boland S, Leysen D, Vandewynckel YP, et al. Treatment of intestinal fibrosis in experimental inflammatory bowel disease by the pleiotropic actions of a local rho kinase inhibitor. *Gastroenterology*. 2017;153:1054–67.
92. Haydont V, Riser BL, Aigueperse J, Vozenin-Brottons MC. Specific signals involved in the long-term maintenance of radiation-induced fibrogenic differentiation: a role for CCN2 and low concentration of TGF- $\beta$ 1. *Am J Physiol Cell Physiol*. 2008;294:C1332–41.

## Publisher's Note

Springer Nature remains neutral with regard to jurisdictional claims in published maps and institutional affiliations.